Pharmacokinetics of the cardioprotective drug dexrazoxane and its active metabolite ADR-925 with focus on cardiomyocytes and the heart

Eduard Jirkovský, Anna Jirkovská, Jan Bureš, Jaroslav Chládek, Olga Lenčová, Ján Stariat, Zuzana Pokorná, Galina Karabanovich, Jaroslav Roh, Petra Brázdová, Tomáš Šimůnek, Petra Kovaříková and Martin Štěrba

Department of Pharmacology, Faculty of Medicine in Hradec Králové, Charles University, Šimkova 870, Hradec Králové, 500 03, Czech Republic.

(E.J., J.C. O.L-P., Z.P. P.B., M.Š.)

Department of Biochemical Sciences, Faculty of Pharmacy in Hradec Králové, Charles University, Akademika Heyrovského 1203, 500 05 Hradec Králové, Czech Republic.

(A.J., T.Š.)

Department of Pharmaceutical Chemistry and Pharmaceutical Analysis, Faculty of Pharmacy in Hradec Králové, Charles University, Akademika Heyrovského 1203, 500 05 Hradec Králové, Czech Republic.

(J.B., J.S., P.K.)

Department of Inorganic and Organic Chemistry, Faculty of Pharmacy in Hradec Králové, Charles University, Akademika Heyrovského 1203, 500 05 Hradec Králové, Czech Republic.

(G.K., J.R.)

JPET Fast Forward. Published on December 22, 2017 as DOI: 10.1124/jpet.117.244848
This article has not been copyedited and formatted. The final version may differ from this version.

Running title page

a) Running Title:

DEX metabolism *in vitro* and *in vivo*

b) Corresponding authors[$]:

Dr. Martin Štěrba

Faculty of Medicine in Hradec Králové

Charles University

Šimkova 870

500 03 Hradec Králové

Czech Republic

Tel.: +420 495 816 312; Fax: +420 495 513 597

E-mail: sterbam@lfhk.cuni.cz

Dr. Petra Kovaříková

Faculty of Pharmacy in Hradec Králové

Charles University

Akademika Heyrovského 1203

500 05 Hradec Králové

Tel.: +420 495 067 236

Czech Republic

E-mail: petra.kovarikova@faf.cuni.cz

c) Counts:

Number of text pages: 58

Number of tables: 3

Number of figures: 9

Number of references: 53

Number of words in the abstract: 246

Number of words in the introduction: 720

Number of words in the discussion: 1685

Supplementary material: Supplementary Figure 1, Supplementary Figure 2, Supplemental Method.

d) Abbreviations:

ANT – anthracycline antibiotics; CV – coefficient of variation; DEX – dexrazoxane; ISV – inter-subject variability; NCA – non-compartmental analyses; NVCM – neonatal rat ventricular cardiomyocytes; % RSE – percent of relative standard error; RVPC – residual variability in plasma concentrations.

e) Section:

Metabolism, Transport, and Pharmacogenomics

Abstract

Dexrazoxane (DEX), the only cardioprotectant approved against anthracycline cardiotoxicity, has been traditionally deemed to be a prodrug of the iron-chelating metabolite ADR-925. However, pharmacokinetic profile of both agents, particularly with respect to the cells and tissues essential for its action (cardiomyocytes/myocardium), remains poorly understood. The aim of this study is to characterize the conversion and disposition of DEX to ADR-925 *in vitro* (primary cardiomyocytes) and *in vivo* (rabbits) under conditions where DEX is clearly cardioprotective against anthracycline cardiotoxicity. Our results show that DEX is hydrolyzed to ADR-925 in cell media independently of the presence of cardiomyocytes or their lysate. Furthermore, ADR-925 directly penetrates into the cells with contribution of active transport, and detectable concentrations occur earlier than after DEX incubation. In rabbits, ADR-925 was detected rapidly in plasma after DEX administration to form sustained concentrations thereafter. ADR-925 was not markedly retained in the myocardium, and its relative exposure was 5.7-fold lower than for DEX. Unlike liver tissue, myocardium homogenates did not accelerate the conversion of DEX to ADR-925 *in vitro* suggesting that myocardial concentrations *in vivo* may originate from its distribution from the central compartment. The pharmacokinetic parameters for both DEX and ADR-925 were determined by both NCA and population pharmacokinetics (including joint parent-metabolite model). Importantly, all determined parameters were closer to human than to rodent data. The present results open venues for the direct assessment of the cardioprotective effects of ADR-925 *in vitro* and *in vivo* to establish whether DEX is a drug or prodrug.

Introduction

Dexrazoxane (DEX, Fig. 1) is the only cardioprotective agent approved for clinical use against cardiotoxicity induced by anthracycline (ANT) anticancer agents (Sterba et al., 2013; Vejpongsa and Yeh, 2014a), and besides that it is also approved for treatment of accidental anthracycline extravasation (Hasinoff, 2006; Langer, 2010). Over the decades of its preclinical development, it has been documented that the cardioprotective effects of DEX are robust in all species tested irrespectively of the ANT derivative (Sterba et al., 2013). Furthermore, clinical efficacy has been firmly established in numerous trials and by their meta-analyses (van Dalen et al., 2011; Vejpongsa and Yeh, 2014a; Hutchins et al., 2017).

DEX is traditionally believed to be a prodrug that is metabolized to an active metabolite - ADR-925 via two intermediate hydrolytic products (termed B and C, Fig. 1). The first step is catalyzed by dihydropyrimidase (initial single ring-opening step), while second step to ADR-925 is catalyzed by dihydroorotase. ADR-925 is deemed to protect cardiomyocytes from ANT-induced oxidative damage by chelating intracellular iron (Hasinoff et al., 1998; Cvetkovic and Scott, 2005). Although this "ROS and iron" hypothesis is very popular, numerous concerns have been raised over the last decade (Sterba et al., 2013). Some experts have questioned even the fundamental concept of DEX action as a prodrug (Hasinoff and Herman, 2007), and further evidence suggests that DEX may protect the heart by catalytic inhibition of topoisomerase IIβ (Lyu et al., 2007; Vejpongsa and Yeh, 2014a; Lencova-Popelova et al., 2016).

It is noteworthy that despite several important contributions (Hasinoff et al., 1998; Hasinoff and Aoyama, 1999a; Hasinoff and Aoyama, 1999b; Schroeder et al., 2002; Schroeder et al., 2003; Schroeder and Hasinoff, 2005; Schroeder et al., 2005), understanding the metabolism of DEX to its putative active metabolite ADR-925 is still considerably limited. This becomes particularly apparent when attempting to put the pharmacodynamics of DEX on a solid

pharmacokinetic ground (Sterba et al., 2013). Clinical data on the metabolism of DEX to ADR-925 are extremely sparse. There is only a single small clinical trial (Schroeder et al., 2003) where ADR-925 was systematically determined in plasma. Unfortunately, DEX was part of an atypical chemotherapeutic combination with high-dose etoposide, the number of patients was limited and the calculated half-life of DEX was longer compared to values commonly reported elsewhere (Cvetkovic and Scott, 2005). Most data from animal experiments were obtained by the Hasinoff group, and all *in vivo* experiments published *in extenso* used only rats (Schroeder and Hasinoff, 2002; Schroeder and Hasinoff, 2005). Moreover, ADR-925 concentrations in the myocardium, where its cardioprotective action should occur, are not completely described. The only available data come from the latter study where concentrations of ADR-925 were determined in a single time point (different for DEX and ADR-925 administration). In addition, the translatability of these *in vivo* findings may not be straightforward due to the strikingly higher elimination rate of DEX in rodents (rats and mice) compared to humans (Hasinoff et al., 1998).

DEX metabolism has also been studied *in vitro* with isolated cardiomyocytes and hepatocytes (Schroeder et al., 2005). However, its concentrations were determined in cell culture media but not within the intracellular compartment where the cardioprotective effects of ADR-925 should occur. Indeed, the relatively polar ADR-925 need not penetrate easily out of the cells, which may make the precise evaluation of DEX metabolism difficult. Furthermore, experiments performed with DEX in cardiomyocytes were short (2 hours), and concentrations of ADR-925 have not been determined. Hence, it remains unknown whether the putative active metabolite achieves markedly prolonged intracellular concentrations in cardiomyocytes, which can be essential for the cardioprotective efficacy of DEX.

Thus, a plasma concentration-time profile of the putative active metabolite (ADR-925) under standard conditions when DEX is administered as a single agent in a clearly cardioprotective

schedule remains unknown. In addition, information on concentration-time profiles of both DEX and ADR-925 in the heart and cardiomyocytes (*i.e.*, at the site of drug action) is missing. Therefore, it is uncertain whether and to what extent DEX is metabolized in the heart and cardiomyocytes, and whether ADR-925 can effectively penetrate this compartment from cell media and circulation.

The aim of the present study is to thoroughly investigate the metabolism of DEX to ADR-925 *in vitro* and *in vivo* on the schedule in which the drug is clearly cardioprotective, with a particular focus on cardiomyocytes and the heart.

Materials and Methods

Drugs and chemicals

For HPLC analysis, gradient grade methanol (MeOH) was purchased from Merck (Darmstadt, Germany). Ammonium formate, 1,2-bis(3,5-dioxopiperazin-1-yl)ethane ($I.S._{DEX}$), 1,3-diaminopropane-N,N,N,N-tetraacetic acid ($I.S._{ADR-925}$) were obtained from Sigma–Aldrich (Schnelldorf, Germany). Milli-Q water was produced by a Millipore purification system (Schwalbach, Germany).

For cell culture experiments, Dulbecco's modified Eagle's medium containing the nutrient mixture F-12 (DMEM/F12), penicillin/streptomycin solution (5000 U/mL; P/S) and sodium pyruvate solution (100 mM; PYR) were purchased from Lonza (Verviers, Belgium). Horse serum (HS) and fetal bovine serum (FBS) were purchased from Sigma-Aldrich or Biosera (Nuaille, France) and were heat-inactivated prior to use (56 °C, 30 minutes). For isolation of cardiomyocytes, collagenase type II (Thermo Fisher Scientific, Waltham, USA) and pancreatin (Sigma-Aldrich) were used. Other chemicals used for *in vitro* and *in* vivo experiments (*e.g.*, constituents of various buffers) were purchased from Sigma–Aldrich or Penta (Prague, Czech Republic). Solutions of DEX and ADR-925 for all *in vitro* experiments were prepared as 1000x concentrated stock solutions in DMSO.

DEX (MW = 268 g/mol) was obtained from Huaren Chemicals (Changzhou, China). Cardioxane (dexrazoxane, Clinigen Healthcare, Burton-on-Trent, UK) was used for *in vivo* pharmacokinetic studies. The racemic form of ADR-925 (ICRF-198) (MW = 304 g/mol) was prepared in house; for a full description of the procedure, see the Supplementary Methods. Ketamine (Narketan, Vétoquinol, Lure, France), midazolam (Midazolam Torrex, Chiesi Pharmaceuticals, Wien, Austria) and pentobarbital (Sigma-Aldrich) were used for anesthesia.

Isolation of rat cardiomyocytes and *in vitro* pharmacokinetic experiments

Neonatal rat ventricular cardiomyocytes (NVCM) have been used for *in vitro* pharmacokinetic studies because this is one of the most established and extensively used models for the *in vitro* study of cardioprotective effects of DEX (Hasinoff, 2002; Hasinoff et al., 2003a; Simunek et al., 2008; Jirkovska-Vavrova et al., 2015). In addition, this system was previously employed in the initial evaluation of DEX metabolism (Schroeder et al., 2005). NVCM were isolated from 1–3-day-old Wistar rats as described previously (Vavrova et al., 2013). Briefly, neonatal hearts were minced in ADS buffer (1.2 mM $MgSO_4.7H_2O$; 116 mM NaCl; 5.3 mM KCl; 1.13 mM $NaH_2PO_4.H_2O$; 20 mM HEPES, pH 7.4) on ice and serially digested at 37 °C with collagenase type II (65 U/mL) and pancreatin (0.4 mg/mL). To minimize non-myocyte cell contamination, a 2-hour pre-plating period (approx. 20 hearts per 150 mm Petri dish) was used before plating the cells on gelatine-coated 60-mm Petri dishes at a density of 2 x 10^5 cells per cm^2. NVCM were cultured at 37 °C in a 5 % CO_2 atmosphere in DMEM/F12 medium supplemented with 10 % HS, 5 % FBS, 4 mM PYR and 1 % P/S (pH 7.4). After 40 hours, the medium was changed to DMEM/F12 supplemented with 5 % FBS, 4 mM PYR and 1 % P/S. For all experiments, the medium was changed to serum- and pyruvate-free DMEM/F12 with 1 % P/S. The use of experimental animals for primary cell culture preparation has been approved by the Animal Welfare Committee of the Faculty of Pharmacy, Charles University.

For investigation of DEX metabolism to ADR-925, NVCM (4.8×10^6 cells) were incubated with 100 μM DEX. This DEX concentration has been repeatedly shown to be protective against ANT toxicity in this cell model (Hasinoff, 2002; Adamcova et al., 2007; Jirkovska-Vavrova et al., 2015). Incubation in the same setting was performed with ADR-925 (100 μM) to determine the ability of the metabolite to penetrate into NVCM. After 3, 6, 9, 12 and 24 hours of incubation in separate dishes with the compounds, samples of the cell culture media were taken, and NVCM were briefly washed twice with PBS at 4 °C, harvested by cell scraping and

centrifuged (700 x g; 10 minutes; 4 °C). Incubations of both compounds with cell-free culture medium were performed to determine their chemical degradation under these conditions. To investigate the possible involvement of active transport of ADR-925 to NVCM, its concentration inside the cells was determined after a 24-hour incubation with the compound at concentrations of 100, 300 and 1000 μM ADR-925 at both 4 and 37 °C. All samples of cell culture media and dry cell pellets were shock-frozen in liquid nitrogen immediately after collection and kept at -80 °C until their analysis. All experiments were performed in quadruplicate.

To determine the contribution of NVCM to conversion of DEX to ADR-925, the lysates of freshly harvested NVCM (4.8×10^6 cells) were used. Pellets of the cells were resuspended in 400 μL of ADS buffer with DEX (100 μM) and sonicated (5 second stroke). The cell-free ADS buffer supplemented with the drug served as a control. The mixture was incubated for 24 hours in dark with slow shaking (37 °C). DEX and ADR-925 concentrations were determined at selected time points (0, 1, 3, 6 and 24 hours) in 50 μL samples of supernatant (3 minutes, RT, 5 000 x g) obtained from the incubation mixture. Internal standards were added, and the samples were treated with 300 μL of ice-cold MeOH, vortexed and centrifuged (2 minutes, 4 °C, 10 000 x g). Final supernatants were filtered through a 0.22 μm porosity filter and immediately analyzed by HPLC-MS.

In vivo pharmacokinetic experiments in rabbits

All *in vivo* experiments and procedures were approved and supervised by Animal Welfare Committee of the Faculty of Medicine in Hradec Kralove, Charles University. Chinchilla male rabbits (n = 30, ~3.8 kg) were randomized into 6 groups (n = 5 each) and fasted overnight before the experiment. Four groups received a single dose of DEX (60 mg/kg, *i.p.*), and the

experiment was terminated at different time points after drug administration: 0.5, 3, 6 and 12 hours. The other two groups of rabbits received ADR-925 at the same dose (60 mg/kg) in 30-minutes *i.v.* infusion into the marginal ear vein to describe the pharmacokinetics of ADR-925 alone, and the experiment was terminated 3 and 12 hours after the start of the infusion. The particular DEX dose and route of administration have been repeatedly shown to provide significant cardioprotection against chronic ANT cardiotoxicity in rabbits when administered 0.5 hours before each ANT dose (Simunek et al., 2004; Popelova et al., 2009; Jirkovsky et al., 2013), and is based on the upper limit of DEX dose previously used in humans cardioprotective study (Swain and Vici, 2004) and also for treatment of ANT extravasation(Kane et al., 2008), *i.e.* the ratio 1:20 to ANT dose (3 mg/kg). The *i.p.* route of administration has been typically used in most cardioprotective experiments in small laboratory animals including rabbits to avoid possible difficulties with repeated administration of both studied agents *i.v.*. The rabbit model was among the first employed to study the cardioprotective effects of DEX *in vivo* and until today, it is one of the best established models providing constantly reliable data (Herman and Ferrans, 1998; Sterba et al., 2013).

Blood samples (≈ 1 mL) were collected from the contralateral ear vein at selected time points (5 minutes–12 hours) after drug administration into BD Vacutainers (Becton Dickenson and Company, Plymouth, UK) containing lithium heparin. Plasma samples were harvested immediately, shock-frozen in liquid nitrogen and stored at -80 °C until analysis.

For drug administration and blood sampling, light anesthesia was induced in rabbits with a mixture of ketamine (25 mg/kg, *i.m.*) and midazolam (2.5 mg/kg, *i.m.*); sedation was then maintained with midazolam when needed. The blood withdrawn from the animals was compensated with an appropriate volume of sterile saline. Urine was collected throughout the experiment, volumes were determined and samples were frozen in liquid nitrogen and stored in -80 °C until analyzed.

At the defined time points, rabbits were overdosed with pentobarbital. The heart was rapidly excised, briefly retrogradely perfused with ice-cold saline and dried with gauze. Left ventricles were dissected and shock frozen in liquid nitrogen. Similarly, the liver and soleus muscle were also collected and frozen in liquid nitrogen. In addition, the volume of urine in the urinary bladder was determined, and urine samples were collected and frozen for analysis.

To determine the effects of tissue homogenates on DEX conversion to ADR-925, freshly harvested rabbit LV myocardium and liver obtained from 2 rabbits were used. Samples were homogenized in 5 volumes of ADS buffer on ice in a glass/PTFE Potter-Elvehjem tissue grinder. Freshly prepared homogenates were diluted with ADS buffer to a final volume of 1 mL to prepare homogenate samples containing two different amounts of the tissue (10 and 100 mg per sample). DEX in a final concentration of 100 μM was added, and this mixture was incubated for 24 hours in dark with slow shaking (37 °C, n = 4 in each tissue amount). The tissue-free ADS buffer supplemented with the drug served as a control. DEX and ADR-925 concentrations were determined at selected time points (0, 1, 3, 6 and 24 hours) in 20 μL of supernatant (3 minutes, RT, 5 000 x g) obtained from the incubation mixture. Internal standards were added to the collected samples, and the samples were treated with 180 μL of ice-cold MeOH, vortexed and centrifuged (2 minutes, 4 °C, 10 000 x g). Final supernatants were filtered through a 0.22 μm porosity filter and immediately analyzed. In addition, DEX (100 μM) was incubated in blank rabbit plasma at 37 °C to examine conversion of DEX to ADR-925 in this material *in vitro* using similar experimental design as described for tissue homogenates.

Determination of DEX and ADR-925 concentrations in biological samples

A previously described HPLC-MS method (Kovarikova et al., 2013) was adapted and validated to determine DEX and ADR-925 concentrations in samples obtained from *in vitro* and *in vivo* experiments. However, validation of this method (according to FDA guidelines) for

simultaneous determination of both DEX and ADR-925 besides the intermediate hydrolytic products B and C was not possible and therefore the intermediates B and C were not followed in this study. Briefly, the analyses were performed on an LC 20A Prominence (Shimadzu, Duisburg, Germany) chromatographic system coupled on-line with LCQ Advantage Max mass spectrometer (Thermo Finnigan, San Jose, USA). Synergi Polar-RP column (150 mm × 3 mm, 4 μm; Phenomenex, Torrance, USA) was used as a stationary phase. The mobile phase composed of components A (5 % MeOH in 2 mM ammonium formate solution, without pH adjustment) and B (MeOH) was employed in the following gradient: 0–7 minutes (0 % B), 7–8 minutes (0–50 % B), 8–22 minutes (50 % B), 22.0–22.1 minutes (50–0 % B), 22.1–30.0 minutes (0 % B). A mobile phase flow rate of 0.15 mL/min, a column oven temperature of 25 °C, the injection volume of 10 μL and an autosampler temperature of 4 °C were used for analysis. ESI in positive mode was used, and quantification was performed in SRM mode: DEX ($[M+H]^+$ at *m*/*z* 269 → *m*/*z* 155), $I.S._{DEX}$ ($[M+H]^+$ at *m*/*z* 255 → *m*/*z* 141), ADR-925 ($[M+K]^+$ at *m*/*z* 343 → *m*/*z* 299) and $I.S._{ADR\text{-}925}$ ($[M+K]^+$ at *m*/*z* 345 → *m*/*z* 301).

Both internal standards were added to all biological samples before treatment. Pellets (4.8×10^6 NVCM) were precipitated with ice-cold MeOH (300 μL) and homogenized using a Bio–vortex mixer (BioSpec Products, Bartlesville, USA) for 30 s and then in an ultrasonic bath. The samples were centrifuged (10 minutes, 4 °C, 16,800 × *g*), and the resulting supernatant was filtered through a 0.45 μm porosity filter (Milex – Hv, Merck-Millipore, Darmstadt, Germany) and analyzed. Cell culture medium samples (50 μL) were diluted with MeOH (20 ×) and directly analyzed. Rabbit plasma (100 μL) was precipitated with ice-cold MeOH (600 μL), vortexed, and after centrifugation (10 minutes, 4 °C, 16,800 × *g*), the supernatants were collected and analyzed. Urine samples were centrifuged, diluted (50-100 x) with a MeOH/water mixture (1:1, v/v) and directly analyzed. Tissues were pulverized under liquid nitrogen, and samples (≈ 100 mg) of each tissue were precipitated with ice-cold methanol (500 μL) and

homogenized using an Ultraturax homogenizer (IKA, Staufen, Germany). After centrifugation (10 minutes, 4 °C, 16,800 × *g*), the supernatants were collected and analyzed.

For each biological material, the method was validated according to the U.S. Food and Drug (FDA) Administration Guidance for Industry: Bioanalytical Method Validation (2001). The linearity of the methods were proven within following concentration ranges: 4–80 pmol/10^6 NVCM and 7–70 pmol/10^6 NVCM for DEX and ADR-925, respectively; 8–100 μM in cell culture medium and ADS buffer (both compounds); 2–340 μM (DEX) and 1–100 μM (ADR-925) in plasma; 15–1500 μM in urine (both compounds) and 3.7–200 nmol/g and 1.6–16 nmol/g per wet tissue weight for DEX and ADR-925, respectively. The samples containing higher concentrations of the analytes were appropriately diluted to fit the relevant concentration range. The applicability of this approach was proved by testing the dilution integrity. Precision and accuracy for all biological materials were ≤ 15 and 20 % for all concentrations and LLOQ, respectively, and thus meet FDA requirements.

Pharmacokinetic analysis of data from *in vivo* experiments

Standard non-compartmental analysis was performed using Kinetica software (version 4.0, Thermo Fisher Scientific Inc., USA). The nonlinear mixed-effects modeling approach was used with pharmacokinetic parameters estimated by the Stochastic Approximation Expectation Maximization algorithm coupled with the Markov Chain Monte Carlo procedure (SAEM-MCMC) as implemented in the software Monolix (version 4; Lixoft, France). The consecutive steps of the pharmacokinetic analysis are as follows:

Naive pooled data (NPD) approach. The concentration-time data of 20 animals subjected to destructive sampling after a single dose of DEX *i.p.* were naive pooled, and the geometric mean concentration-time profiles of plasma DEX and ADR-925 were subjected to standard non-compartmental analysis (NCA). The same approach was used to calculate model-independent

parameters of plasma ADR-925 from 96 assayed concentrations after *i.v.* infusion of the metabolite to 9 animals. The cumulative amounts of DEX and ADR-925 excreted in urine by all animals were plotted against time, the parameters of one-phase association curve were fitted to the data, and the mean total amounts excreted as unchanged drug and/or ADR-925 were calculated as asymptotes. The fractions of the dose excreted as unchanged drug and/or the metabolite and renal clearances were computed.

The standard two-stage (STS) method. To improve the accuracy of the PK naive pooled data biased by animals terminated at the time of unfinished metabolization and elimination processes, PK parameters after both DEX and ADR-925 administration were estimated by NCA using data of the subgroup of the animals with entire 12-hour sampling (n = 5 for each compound). The total urinary excretions and renal clearances were calculated without extrapolation.

Population modeling. Logarithms of molar DEX and ADR-925 concentrations in plasma and of their urinary molar quantities improved the precision of parameter estimates and were used throughout. Inter-animal variability was evaluated with the use of an exponential error model, and residual variability was evaluated with an additive error model on the logarithmic scale. First, separate models were built up that described DEX plasma concentration and the amount of DEX excreted in urine after its *i.p.* injection (Model 1), and for plasma and urinary data of ADR-925 after *i.v.* infusion of the metabolite (Model 2). Finally, a joint model was elaborated that simultaneously described DEX and ADR-925 plasma concentrations and urinary amounts after the *i.p.* injection of the parent compound (Model 3).

The compartmental models were parameterized in terms of volume of distribution (central and peripheral), inter-compartmental clearance, total and renal clearances, and, in case of the joint Model 3, the metabolic clearance of DEX to ADR-925. The models for DEX assumed first-

order absorption without a lag time, and the absolute bioavailability F = 1 was assumed based on the rapid appearance of DEX in plasma after administration.

Urinary recovery of the *i.v.* dose of ADR-925 was shown to be complete in this study. Therefore, the metabolite volumes of distribution were identifiable in Model 3, which included the data on urinary excretion of ADR-925. The predictive performance of the models was evaluated using goodness-of-fit plots and the distribution of observations with respect to the model-predicted median profiles and 90 % prediction intervals, *i.e.,* the visual predictive checks (VPC). Finally, empirical Bayes estimates of each parameter were obtained, and secondary pharmacokinetic characteristics were calculated.

In the case of tissue concentrations, the mean value and variance of the AUC were calculated with the help of the package PK, version 1.3-3, named Basic Non-Compartmental Pharmacokinetics (Jaki et al., 2010).

Data analysis and presentation

Data are shown as the mean ± SD unless stated otherwise. Pearson and Spearman correlation analyses, linear regression analyses, and statistical significance differences (using One-Way ANOVA with Holm-Sidak's or ANOVA on Ranks with Dunn's post hoc test) were determined according to the data character using software SigmaStat 3.5 (SPSS, USA).

JPET Fast Forward. Published on December 22, 2017 as DOI: 10.1124/jpet.117.244848
This article has not been copyedited and formatted. The final version may differ from this version.

Results

Distribution of DEX/ADR-925 in isolated rat cardiomyocytes and conversion of DEX to ADR-925

DEX and ADR-925 concentrations were determined in cell culture medium and inside NVCM after their incubation with DEX (100 μM, up to 24 hours). In the culture medium with NVCM, DEX concentrations gradually fell to ≈ 30 μM after 24 hours (Fig. 2A), while ADR-925 concentrations steadily increased from the 3rd hour to exceed the concentrations of the parent compound between the 12th and 24th hours, reaching ≈ 45 μM at the end of the experiment (Fig. 2A). Almost identical results were obtained in culture media without NVCM (Fig. 2A), which indicates that DEX conversion to ADR-925 is related to spontaneous hydrolysis rather than cardiomyocyte metabolic activity. Inside NVCM, DEX was determined after 3 hours of incubation, with its peak value in the 6th hour. The concentrations of DEX gradually declined thereafter but were detectable until the end of the incubation (Fig. 2B). In the same experiment, ADR-925 concentrations inside the cells were first detected in the 9th hour and then progressively increased until the end of experiment (24 hours), where it achieved concentrations approximately twice as high as those of DEX (Fig. 2B). Direct incubation of NVCM with ADR-925 (in the same concentrations as DEX, 100 μM) resulted in a slower penetration of this agent into the intracellular compartment compared to DEX, but the concentrations were considerably higher than those formed in the previous experiment after incubation of the cells with DEX. The concentrations of ADR-925 then gradually increased in time to match the concentrations of DEX determined in the previous experiment in the 9th hour (Fig. 2B), and a further increase of ADR-925 concentration continued until the end of the incubation. Intracellular concentrations of ADR-925 were almost double throughout this experiment compared to the concentrations of ADR-925 determined after DEX incubation.

In further experiments, we wanted to examine whether and to what extent active transport contributes to the penetration of the relatively polar metabolite ADR-925 into NVCM. Therefore, these cells were incubated with ADR-925 (100–1000 μM) at 4 °C or 37 °C for 24 hours. The result of this experiment showed that the penetration of ADR-925 into the cells is temperature-dependent, as the concentrations inside the cells were significantly lower at 4 °C compared to 37 °C, which indicates contribution of an active type of transport (Fig. 2C). On the other hand, the experiment performed with the higher concentration did not show any ceiling effect, which suggests that the transport is not saturable in the tested concentration range.

To directly assess the role of intracellular enzymes in DEX metabolism to ADR-925, 100 μM DEX was incubated for 24 hours with NVCM homogenate or the corresponding ADS buffer. The results showed that NVCM homogenate (Fig. 2D) did not have any significant effect on the formation of ADR-925 from DEX, and the concentrations were comparable with those determined in the buffer (Fig. 2D).

DEX metabolism and disposition in rabbits

Plasma concentrations and urinary excretion of DEX and ADR-925

The rate of absorption of DEX (60 mg/kg) administered as a single intraperitoneal bolus to rabbits was high (Fig. 3A). The highest plasma concentrations of DEX were observed in individual time profiles between the 5th and 30th minute after the injection with the median time interval of 10 minutes. The geometric mean concentration of plasma DEX peaked at the 10th minute, and its decrease from the c_{max} (337 μM) was apparently biphasic, leaving only 1.7 % of the c_{max} concentration at the end of the twelve-hour sampling interval.

The metabolite was detected in all plasma samples collected at the 5th minute, but its concentrations (Fig. 3A) were relatively lower compared to the parent compound. Its geometric mean of concentration increased gradually until the 45th minute, reaching the c_{max} (35.6 μM).

A broad plateau was then observed on the mean concentration-time profile of ADR-925 between the 45th minute and the 5th hour. After this time interval, the mean concentration of the metabolite showed a monotonous decline in parallel with that of DEX. The residual metabolite concentrations at the 12th hour corresponded to 14 % of the c_{max}. The slow formation of ADR-925 in plasma observed in the curve of the mean concentrations followed with a plateau was not the effect of pooling of the data from different animals as it was also found on the concentration-time profiles of individual animals (data not shown). The median time to the maximum concentration was 2 hours (0.5–8 hours) in 13 rabbits that were sampled over a sufficiently long interval to reach the c_{max}.

In another experiment, ADR-925 (60 mg/kg) was infused intravenously to rabbits over 30 minutes to follow the distribution and elimination kinetics of the metabolite from plasma. The highest concentrations of ADR-925 in plasma were observed at the end of the infusion (30 minutes) with the exception of one animal (20 minutes). The geometric mean of the c_{max} was found to be 557 μM. Similar to DEX, the decline of the mean plasma concentrations of ADR-925 exhibited a biphasic pattern and, after 12 hours, only 0.2 % of the c_{max} remained in plasma (Fig. 3B).

The cumulative urinary excretion of DEX and ADR-925 followed for 12 hours after a bolus dose of 60 mg/kg DEX *i.p.* is shown in Fig. 4A. The mean total amounts of DEX and ADR-925 excreted via the urine, estimated as asymptotes by nonlinear regression, were 309 μmol and 103 μmol, respectively. The amounts of the parent drug, metabolite, and their sum in the urine estimated from all animals (NPD) represent 35.5 % (DEX), 11.9 % (ADR-925) and 47.4 % (DEX + ADR-925) of the administered dose, respectively. Similarly, in the subgroup of 5 animals with urine collected over the entire 12 hours, the total recoveries were

JPET Fast Forward. Published on December 22, 2017 as DOI: 10.1124/jpet.117.244848
This article has not been copyedited and formatted. The final version may differ from this version.

35.7 ± 11.1 % (DEX), 11.0 ± 4.3 % (ADR-925) and 46.6 ± 10.9 % (DEX + ADR-925) of the dose.

A vast majority of the intravenously infused dose of ADR-925 was excreted unchanged in urine, supporting the view that renal excretion is a predominant elimination pathway for this metabolite (Fig. 4B). The mean total urinary excretion and recovery of ADR-925 estimated from all naive-pooled animals were 664 μmol and 89.5 %, respectively. Nonlinear regression may have underestimated the total amount of the drugs excreted by the kidneys due to the influence of data from animals with shorter intervals of collection. In the subgroup of the animals within the 12-hour collection interval, the mean urinary recovery of the infused dose of the metabolite achieved 98 ± 6 %, indicating that the excretion was practically complete.

Non-compartmental analysis

Pharmacokinetic parameters calculated by non-compartmental analysis (NCA) are summarized in Table 1. Due to the batch design of the experiment, *i.e.*, the variable length of the sampling interval in subgroups of animals, NCA could be applied on the geometric mean of concentration-time profile obtained from all naive-pooled animals (n = 20) and on individual profiles of animals with 12-hour sampling (n = 5). Blood sampling over 12 hours was adequate for the description of plasma pharmacokinetics of DEX and ADR-925 in both studies. After a bolus dose of DEX, the extrapolated parts of the AUCs were less than 4 % (DEX) and 10 % (ADR-925), with the exception of one individual concentration-time profile of ADR-925 where the extrapolated part of the AUC was 23 %. After *i.v.* infusion of ADR-925, extrapolation beyond the 12^{th} hour accounted for less than 1 % of the AUC.

In general, there was good agreement between the results of the NCA analysis of naive-pooled concentration-time data from all animals and the two-stage approach used in five animals sampled over 12 hours (Table 1). Two exceptions were the c_{max} of DEX and t_{max} of the

metabolite after DEX injection. Obviously, the single-point pharmacokinetic characteristics c_{max} and t_{max} are more variable between animals, and their estimates are more prone to bias. In addition, the broad plateau on the ADR-925 mean concentration-time profile explains the discrepancy regarding its t_{max}.

The fraction of the DEX dose metabolized to ADR-925 (11 %) was calculated assuming that the absolute bioavailability of DEX equals one (F = 1) and that renal excretion is the sole elimination pathway for the metabolite after DEX injection, which is supported by our data after infusion of ADR-925. As judged from the ratio of the mean AUCs (parent/metabolite) of 3.2, DEX was the quantitatively prevailing compound in plasma.

The renal clearance of ADR-925 after DEX injection was approximately two-fold lower compared to infusion of ADR-925. Of note, the c_{max} of plasma ADR-925 was 15-fold higher at the end of the *i.v.* infusion of ADR-925, and the concentrations remained markedly higher during the first post-infusion hour compared to the maximum concentrations of ADR-925 metabolically formed after DEX injection. The finding of the concentration-dependent renal clearance complicated the comparison of the MRT and $t_{1/2}$ values of ADR-925 in both studies. The $MRT_{i.v.}$ of ADR-925 (2.5 hours), calculated as ($MRT_{metabolite}$ - MRT_{parent}) after DEX injection, was thus higher than the $MRT_{i.v.}$ of ADR-925 after infusion of ADR-925 (1.6 hours), obtained as the difference ($MRT_{inf} – T_{inf}/2$).

Population pharmacokinetic analysis

A schematic representation of the separate models for DEX and ADR-925 is given in Fig. 5A and Fig. 5B, respectively. After *i.p.* injection, disposition of DEX in plasma was best described by a two-compartment open model with first-order absorption and elimination without a time lag (Model 1). The final model for ADR-925 was a two-compartment model with zero-order input via *i.v.* infusion and first-order elimination (Model 2). In the joint parent-metabolite model

(Model 3; Fig. 5C), formation of ADR-925 from plasma DEX was modeled as a first-order process, and the amount of the metabolite recovered in urine was taken as representative of its overall quantity produced by metabolism. The central and peripheral volumes of distribution of the metabolite were added to achieve the best description of the combined data from DEX and ADR-925.

The statistical summary of Bayesian post hoc estimates of individual pharmacokinetic parameters produced by Models 1, 2 and 3 are presented in the Table 2. The relative standard errors not exceeding 24 % document an adequate precision of estimates for all parameters. Values of clearances and volumes of distribution agreed reasonably well with those from NCA. The joint parent-metabolite model also allowed for determination of the metabolic clearance of DEX (0.045 $L \cdot h^{-1} \cdot kg^{-1}$) and the estimation of secondary pharmacokinetic parameters for DEX presented as a geometric mean: Cl_{tot} = 0.26 $L \cdot h^{-1} \cdot kg^{-1}$, V_{ss} = 0.74 L/kg, $t_{1/2\alpha}$ = 11.5 minutes and $t_{1/2\beta}$ = 131.4 minutes.

The visual predictive performance and goodness-of-fit of the models was good (Fig. 6 and Suppl. Fig. 1). The observed plasma DEX and ADR-925 concentrations fit well within the 5–95 % of prediction intervals. Population mean predicted plasma concentrations adequately describe the central tendencies in concentration-time data. The goodness-of-fit is evident from the scatter plots of observed vs. individual predicted plasma concentrations, calculated by Bayesian estimation (Fig. 6 and Suppl. Figs. 1C, D).

Tissue concentrations of DEX and ADR-925 in rabbits

DEX and its metabolite ADR-925 were also determined in the selected tissues (LV myocardium, liver and soleus muscle) at different time points after DEX administration to rabbits (Fig. 7A–C). Very similar DEX and ADR-925 concentrations (including the overall concentration-time profile) were determined in the LV myocardium and in the liver. The

concentrations of DEX in both tissues were more than double compared to the soleus muscle 30 minutes after drug administration, and they decreased faster than in the muscle. Both in the myocardium and liver, the decrease in DEX concentrations was not accompanied by a proportional increase of ADR-925. In fact, the concentrations of the metabolite remained relatively steady throughout the experiment particularly in the liver, with tendency towards a slow rise in the heart. These data argue against distinct intracellular trapping and cumulation of the relatively polar ADR-925 in this tissue. A different situation was demonstrated in soleus muscle, where the concentrations of the metabolite increased more significantly compared to the decline of DEX. Different concentrations of both drugs in the soleus muscle compared to other tissues could be caused by lower perfusion of the peripheral muscle compared to the myocardium and the liver.

The DEX concentrations determined in plasma at the end of the study showed a very good relationship with the corresponding concentrations found in the tissues in the same time point (Suppl. Fig. 2A-C). However, this was not the case for ADR-925 (Suppl. Fig. 2D-F), where the concentrations in the myocardium and liver tissue showed no significant correlation with the plasma concentrations ($p > 0.05$), and only poor and a surprisingly negative correlation was found in the soleus muscle ($p = 0.021$, $R = -0.513$).

The total exposure of the tissues to DEX and ADR-925 estimated as AUC (Table 3) revealed that after DEX administration, the LV myocardium and liver tissue were exposed to 5.7 and 4.8 times (respectively) higher concentrations of the parent drug compared to ADR-925, whereas the ratio was lower in the soleus muscle (3.5 times). The ratios in the former tissues are significantly higher than that found in plasma (3.2 times).

To directly estimate tissue metabolism of DEX to ADR-925, we incubated LV myocardial and liver homogenates with DEX at 37 °C and determined concentrations of both of these

compounds (Fig. 8A, B). Only a slight decrease of DEX concentrations occurred after 6 hours of incubation with myocardial homogenates, which corresponds with low concentrations of the metabolite. Importantly, the amount of the myocardial tissue in the homogenate had no impact on the results, and the concentrations were very similar as in ADS buffer without tissue homogenate. In contrast, the same experiments performed with liver homogenates documented a significantly accelerated decrease of DEX concentration with a concomitant increase of ADR-925. Because there was also an apparent difference between the samples prepared with a different amount of the liver tissue, it seems that this activity is attributable to content of the tissue and biotransformation enzymes. To estimate whether DEX may also be converted to ADR-925 in plasma more effectively than by simple chemical hydrolysis in the buffer, DEX was incubated in rabbit plasma at 37 °C (Fig. 9). These experiments demonstrated that DEX is converted to ADR-925 in plasma significantly more effectively than in ADS buffer. After 6 hours of incubation, plasma concentrations of DEX decreased by more than 60 %, while in ADS buffer it was approx. 20 %, and the concentrations of ADR-925 rose concomitantly. Interestingly, DEX concentrations in plasma dropped down after 24 hours to negligible values, while ADR-925 concentrations approached 100 μM, suggesting almost complete conversion of DEX to ADR-925 under these conditions. This was not the case in ADS buffer, where the decline of DEX concentrations was approx. 50 % at the same time point with a similar increase of ADR-925 concentrations. Although intermediate metabolites B and C could not be determined in these experiments, their theoretical portion can be approximated based on mass balance as a resting portion on the top of the sum of DEX and ADR-925 (Fig. 9B).

Discussion

This study adds several important pieces into the puzzle of the pharmacokinetics of DEX and its putative active metabolite ADR-925 under well-established experimental conditions in which DEX is known to provide reliable protection from ANT cardiotoxicity. We have documented a slow and progressive rise of intracellular concentrations of ADR-925 in NVCM after DEX incubation. We have proven that ADR-925 can directly, albeit relatively slowly, penetrate from the cell culture medium into cardiomyocytes, and the resulting intracellular concentrations are significantly higher than after incubation of the cells with equimolar DEX concentrations. Our data suggest the contribution of an active transmembrane transport, but particular transporter for ADR-925 remains unknown. According to its chemical structure, one could speculate on involvement of a member of the solute carrier family (SLC) transporters, especially for organic cation/carnitine transporter family (OCTN, SLC22) (Klaassen and Aleksunes, 2010; Tamai, 2013), from which OCTN2 was described to be present in the mouse and human heart (Grube et al., 2006). Of note, we showed that significant non-enzymatic hydrolysis of DEX to ADR-925 already occurs in the culture media, and the rate is faster than in the buffer of corresponding pH. Hence, during 12-hour experiments, the cells are exposed to relatively high concentrations of ADR-925, and in longer experiments, the exposure to the metabolite predominates over DEX. It is noteworthy that NVCM lysate had no significant impact on conversion of DEX to ADR-925. This may imply that a significant part of ADR-925 intracellular concentrations found after incubation with DEX can arise from penetration of ADR-925 from the medium, where it originates by non-enzymatic hydrolysis of the parent compound. The hydrolysis has been described to be promoted by presence of metal-ions (esp. Fe^{2+}, Ca^{2+}, Cu^{2+} and Mg^{2+}) (Buss and Hasinoff, 1995; Buss and Hasinoff, 1997), although in the rather higher concentrations then they are present in the present cell media. On the other hand, Schroeder et al. (2005) previously published that suspension of neonatal cardiomyocytes

accelerated the decrease of DEX concentrations in the medium, which may appear to be in contrast to our findings. However, the interpretation of these results is complicated by short incubation of the cells with DEX (2 hours), resulting in a relatively small decline of DEX concentration, and by a lack of information on ADR-925 formation.

In contrast to DEX, incubation of isolated rat cardiomyocytes with ADR-925 has been previously reported to be unable to protect the cells from doxorubicin toxicity, and one possible explanation was poor penetration of the putative active metabolite into the cells due to its anionic hydrophilic nature (Hasinoff et al., 2003b). However, our data obtained also from rat cardiomyocytes clearly contradict this hypothesis and further contribute to questioning ADR-925 as an active metabolite responsible for DEX-induced cardioprotection (Sterba et al., 2013).

Plasma pharmacokinetic profiles of DEX in rabbits determined in this study are surprisingly close to those reported from clinical trials. Basic pharmacokinetic parameters calculated in this study practically match those reported in patients (in order: our NCA data vs. human data - NCA data if possible): biological half-life of elimination ($t_{1/2\beta}$) 2.0 hours vs. ≈ 2–4 hours (Earhart et al., 1982; Vogel et al., 1987; Hochster et al., 1992; Rosing et al., 1999), total clearance 0.26 vs. ≈ 0.19–0.35 $L \cdot h^{-1} \cdot kg^{-1}$ (Holcenberg et al., 1986; Vogel et al., 1987; Rosing et al., 1999), volume of distribution (V_{ss}) 0.74 vs. ≈ 0.45–1.1 L/kg (Holcenberg et al., 1986; Wiseman and Spencer, 1998), and the recovery of administered DEX dose in urine (as DEX + ADR-925) 47 % vs. 40–48 % (Earhart et al., 1982; Rosing et al., 1999; Tetef et al., 2001). DEX pharmacokinetic in humans was described to be different in pediatric patients and in adults (Holcenberg et al., 1986), and to be linear in broad range of DEX concentrations (Hochster et al., 1992). Our findings in rabbits thus differ considerably from rodents where the elimination of DEX has been reported as 4–6 times faster (Hasinoff et al., 1998; Hasinoff and Aoyama, 1999a). This suggests that rabbit is a valuable animal model to study the cardioprotective effects of DEX not only from a pharmacodynamic (Herman and Ferrans, 1998;

Simunek et al., 2004; Popelova et al., 2009; Jirkovsky et al., 2012) but also from a pharmacokinetic point of view.

The plasma profile of the putative active metabolite (ADR-925) after DEX administration to rabbits was also relatively close to reports from the single human study published so far (Schroeder et al., 2003). In both, the metabolite appeared in plasma in the first sample taken after drug administration and formed a plateau for several hours (≈ 5 hours in rabbits and ≈ 4 hours in humans) with a relatively slow decline until the end of the study. Although the administered doses were not the same in these studies, the range of plasma concentrations of ADR-925 in the plateau phase was similar (≈ 40 μM after 1000 mg/m^2 of DEX in rabbits and 30 μM after 1500 mg/m^2 in patients). Unfortunately, the pharmacokinetic analysis for ADR-925 was not performed in the clinical study, and thus the pharmacokinetic parameters cannot be directly compared. The profile of ADR-925 was also studied in rats after DEX administration (40 mg/kg, *i.v.*) (Schroeder and Hasinoff, 2002). In the latter study, ADR-925 was detected in plasma soon after DEX administration, with a peak of plasma concentrations in the 80th minute (≈ 80 μM) and tended to decrease faster than in rabbits and humans. The short duration of this study (3 hours) did not allow for appropriate evaluation of metabolite elimination. However, the same authors evaluated the pharmacokinetics of ADR-925 after an *i.v.* bolus of either ADR-925 or the intermediate metabolites (B/C) of DEX to rats (Schroeder and Hasinoff, 2005). They observed a rapid decline of ADR-925 with $t_{1/2}$ ≈ 20 min (as estimated from the graphical data) after administration of ADR-925, while an even shorter $t_{1/2}$ (8.3 minutes) was calculated from elimination constants for ADR-925 after administration of intermediate metabolites. This contrasts our data from rabbits, where the $t_{1/2}$ ≈ 100 minutes. Our study has shown that ADR-925 is almost completely eliminated unchanged by the kidney to urine. We have also created a population-based pharmacokinetic model taking into account both parent DEX and ADR-925.

Our study has also systematically described the time course of DEX and ADR-925 tissue concentrations, especially in LV myocardium as the target tissue for cardioprotection. The data from patients are naturally unavailable and besides scarce data from conference abstracts (Mhatre et al., 1983; McPherson et al., 1984), very little information has been published from animal experiments *in extenso* so far (Schroeder and Hasinoff, 2005; Schroeder et al., 2008). As a part of these two studies, myocardial ADR-925 concentrations were described after DEX administration (40 mg/kg, *i.v.*) to rats in the single arbitrary selected time point (after 2.8 or 2-2.5 hours, respectively). However, only the former study also provided concentrations of the parent compound. The concentrations of ADR-925 tended to be significantly higher in these rat studies than in our experiments with rabbits, but direct comparison is difficult due to different dose/route of administration and only discrete information of tissue concentrations in the former studies. As plasma pharmacokinetics of DEX and ADR-925 is markedly different in rodents than in humans and rabbits, tissue concentrations of both compounds may also be affected.

We have studied the metabolism of DEX to ADR-925 in rabbit tissue homogenates to reveal that unlike liver, myocardial tissue does not accelerate DEX hydrolysis and the formation of ADR-925. This is consistent with our *in vitro* results obtained from DEX incubation with NVCM and their lysates and with the study published by Hasinoff et al. (1991). Although the former study struggled with difficulties such as unavailability of appropriate bioanalytical methodology and the incubations were rather short (4 hours), they also found a lack of ADR-925 increase after DEX incubation with porcine heart homogenate, contrary to incubation with the liver homogenate. This may be evidently connected with the high amount and activity of dihydropyrimidase, which catalyzes the first hydrolytic step, in the liver in contrast to myocardial tissue (Hasinoff et al., 1991). Interestingly, we found that DEX was considerably hydrolyzed to ADR-925 by incubation in fresh rabbit plasma under physiological temperature. Hence, it is possible that DEX may be significantly converted to ADR-925 in the circulation,

which may contribute to early detection of ADR-925 after DEX administration in all studies performed so far. The plasma instability of DEX could not confound data in our study because its pre- and analytical parts were designed and validated accordingly. Altogether, these data may imply that the ADR-925 concentrations found inside rat cardiomyocytes and rabbit LV myocardium are determined largely by distribution of ADR-925 or its intermediate hydrolytic products from the circulation, where it could originate both by non- or enzymatic hydrolysis and/or by release from metabolically active organs such as the liver. Differences between correlations of plasma and tissue concentrations of DEX and ADR-925 may be a consequence of different distributions into the intracellular compartments (slower for ADR-925), which correspond with the more hydrophilic nature of ADR-925.

One of the limitations of the present study is the lack of direct information on the two intermediate hydrolytic metabolites B and C. This was caused by difficulties with their appropriate analytical determination besides DEX and ARD-925. However, both intermediate metabolites have been tested previously *in vitro* for cardioprotective properties against ANT cardiotoxicity with negative outcomes (Hasinoff et al., 2003) and therefore they were out of our primal interest. Indirect information on portion of B and C from the plasma hydrolysis experiments suggested their minor appearance.

In conclusion, the present study filled in several important gaps in the pharmacokinetic profile and tissue disposition of the clinically used cardioprotectant DEX to its putative active metabolite ADR-925 in a rabbit model, which shows pharmacokinetic similarities to humans. Importantly, the finding that ADR-925 could directly enter cardiomyocytes opens a venue for direct determination of whether ADR-925 is actually the active metabolite of DEX that is responsible for its cardioprotective effects, as this is now disputed in the literature (Hasinoff and Herman, 2007; Sterba et al., 2013; Henninger and Fritz, 2017).

Acknowledgement

The authors thank Mrs. Klára Lindrová for excellent technical assistance during the experiments.

Authorship Contributions

Participated in research design: Chládek, Jirkovská, Jirkovský, Kovaříková, Lenčová, Šimůnek, Štěrba

Conducted experiments: Brázdová, Bureš, Jirkovská, Jirkovský, Karabanovich, Kovaříková, Lenčová, Pokorná, Roh, Štěrba

Contributed new reagent or analytic tools: Bureš, Karabanovich, Roh, Stariat

Performed data analysis: Bureš, Chládek, Jirkovská, Jirkovský, Kovaříková, Šimůnek, Štěrba

Wrote or contributed to the writing of the manuscript: Brázdová, Bureš, Chládek, Jirkovská, Jirkovský, Kovaříková, Lenčová, Pokorná, Roh, Šimůnek, Štěrba

References

Adamcova M, Simunek T, Kaiserova H, Popelova O, Sterba M, Potacova A, Vavrova J, Malakova J, and Gersl V (2007) In vitro and in vivo examination of cardiac troponins as biochemical markers of drug-induced cardiotoxicity. *Toxicology* **237:**218-228.

Buss JL and Hasinoff BB (1995) Ferrous ion strongly promotes the ring opening of the hydrolysis intermediates of the antioxidant cardioprotective agent dexrazoxane (ICRF-187). *Arch Biochem Biophys* **317:**121-127.

Buss J and Hasinoff B (1997) Metal ion-promoted hydrolysis of the antioxidant cardioprotective agent dexrazoxane (ICRF-187) and its one-ring open hydrolysis products to its metal-chelating active form. *Journal of Inorganic Biochemistry* **68:**101-108.

Cvetkovic RS and Scott LJ (2005) Dexrazoxane : a review of its use for cardioprotection during anthracycline chemotherapy. *Drugs* **65:**1005-1024.

Earhart RH, Tutsch KD, Koeller JM, Rodriguez R, Robins HI, Vogel CL, Davis HL, and Tormey DC (1982) Pharmacokinetics of (+)-1,2-di(3,5-dioxopiperazin-1-yl)propane intravenous infusions in adult cancer patients. *Cancer Res* **42:**5255-5261.

Grube M, Meyer zu Schwabedissen HE, Prager D, Haney J, Moritz KU, Meissner K, Rosskopf D, Eckel L, Bohm M, Jedlitschky G, and Kroemer HK (2006) Uptake of cardiovascular drugs into the human heart: expression, regulation, and function of the carnitine transporter OCTN2 (SLC22A5). *Circulation* **113:**1114-1122.

Hasinoff BB (2002) Dexrazoxane (ICRF-187) protects cardiac myocytes against hypoxia-reoxygenation damage. *Cardiovasc Toxicol* **2:**111-118.

Hasinoff BB (2006) Dexrazoxane use in the prevention of anthracycline extravasation injury. *Future Oncol* **2:**15-20.

Hasinoff BB and Aoyama RG (1999a) Relative plasma levels of the cardioprotective drug dexrazoxane and its two active ring-opened metabolites in the rat. *Drug Metab Dispos* **27:**265-268.

Hasinoff BB and Aoyama RG (1999b) Stereoselective metabolism of dexrazoxane (ICRF-187) and levrazoxane (ICRF-186). *Chirality* **11:**286-290.

Hasinoff BB, Hellmann K, Herman EH, and Ferrans VJ (1998) Chemical, biological and clinical aspects of dexrazoxane and other bisdioxopiperazines. *Curr Med Chem* **5:**1-28.

Hasinoff BB and Herman EH (2007) Dexrazoxane: how it works in cardiac and tumor cells. Is it a prodrug or is it a drug? *Cardiovasc Toxicol* **7:**140-144.

Hasinoff BB, Reinders FX, and Clark V (1991) The enzymatic hydrolysis-activation of the adriamycin cardioprotective agent (+)-1,2-bis(3,5-dioxopiperazinyl-1-yl)propane. *Drug Metab Dispos* **19:**74-80.

Hasinoff BB, Schnabl KL, Marusak RA, Patel D, and Huebner E (2003a) Dexrazoxane (ICRF-187) protects cardiac myocytes against doxorubicin by preventing damage to mitochondria. *Cardiovasc Toxicol* **3:**89-99.

Hasinoff BB, Schroeder PE, and Patel D (2003b) The metabolites of the cardioprotective drug dexrazoxane do not protect myocytes from doxorubicin-induced cytotoxicity. *Mol Pharmacol* **64:**670-678.

Henninger C and Fritz G (2017) Statins in anthracycline-induced cardiotoxicity: Rac and Rho, and the heartbreakers. *Cell Death Dis* **8:**e2564.

Herman EH and Ferrans VJ (1998) Preclinical animal models of cardiac protection from anthracycline-induced cardiotoxicity. *Semin Oncol* **25:**15-21.

Hochster H, Liebes L, Wadler S, Oratz R, Wernz JC, Meyers M, Green M, Blum RH, and Speyer JL (1992) Pharmacokinetics of the cardioprotector ADR-529 (ICRF-187) in escalating doses combined with fixed-dose doxorubicin. *J Natl Cancer Inst* **84:**1725-1730.

Holcenberg JS, Tutsch KD, Earhart RH, Ungerleider RS, Kamen BA, Pratt CB, Gribble TJ, and Glaubiger DL (1986) Phase I study of ICRF-187 in pediatric cancer patients and comparison of its pharmacokinetics in children and adults. *Cancer Treat Rep* **70:**703-709.

Hutchins KK, Siddeek H, Franco VI, and Lipshultz SE (2017) Prevention of cardiotoxicity among survivors of childhood cancer. *Br J Clin Pharmacol* **83:**455-465.

Jaki T, Wolfsegger MJ, and Lawo JP (2010) Establishing bioequivalence in complete and incomplete data designs using AUCs. *J Biopharm Stat* **20:**803-820.

Jirkovska-Vavrova A, Roh J, Lencova-Popelova O, Jirkovsky E, Hruskova K, Potuckova-Mackova E, Jansova H, Haskova P, Martinkova P, Eisner T, Kratochvil M, Sus J, Machacek M, Vostatkova-Tichotova L, Gersl V, Kalinowski D, Muller M, Richardson D, Vavrova K, Sterba M, and Simunek T (2015) Synthesis and analysis of novel analogues of dexrazoxane and its open-ring hydrolysis product for protection against anthracycline cardiotoxicity in vitro and in vivo. *Toxicology Research* **4:**1098-1114.

Jirkovsky E, Lencova-Popelova O, Hroch M, Adamcova M, Mazurova Y, Vavrova J, Micuda S, Simunek T, Gersl V, and Šterba M (2013) Early and delayed cardioprotective intervention with dexrazoxane each show different potential for prevention of chronic anthracycline cardiotoxicity in rabbits. *Toxicology* **311:**191-204.

Jirkovsky E, Popelova O, Krivakova-Stankova P, Vavrova A, Hroch M, Haskova P, Brcakova-Dolezelova E, Micuda S, Adamcova M, Simunek T, Cervinkova Z, Gersl V, and Sterba M (2012) Chronic Anthracycline Cardiotoxicity: Molecular and Functional Analysis with Focus on Nuclear Factor Erythroid 2-Related Factor 2 and Mitochondrial Biogenesis Pathways. *Journal of Pharmacology and Experimental Therapeutics* **343:**468-478.

Kane RC, McGuinn WD, Jr., Dagher R, Justice R, and Pazdur R (2008) Dexrazoxane (Totect): FDA review and approval for the treatment of accidental extravasation following intravenous anthracycline chemotherapy. *Oncologist* **13:**445-450.

Klaassen CD and Aleksunes LM (2010) Xenobiotic, bile acid, and cholesterol transporters: function and regulation. *Pharmacol Rev* **62:**1-96.

Kovarikova P, Pasakova-Vrbatova I, Vavrova A, Stariat J, Klimes J, and Simunek T (2013) Development of LC-MS/MS method for the simultaneous analysis of the cardioprotective drug dexrazoxane and its metabolite ADR-925 in isolated cardiomyocytes and cell culture medium. *J Pharm Biomed Anal* **76:**243-251.

Langer SW (2010) Extravasation of chemotherapy. *Curr Oncol Rep* **12:**242-246.

Lencova-Popelova O, Jirkovsky E, Jansova H, Jirkovska-Vavrova A, Vostatkova-Tichotova L, Mazurova Y, Adamcova M, Chladek J, Hroch M, Pokorna Z, Gersl V, Simunek T, and Sterba M (2016) Cardioprotective effects of inorganic nitrate/nitrite in chronic anthracycline cardiotoxicity: Comparison with dexrazoxane. *Journal of Molecular and Cellular Cardiology* **91:**92-103.

Lyu YL, Kerrigan JE, Lin CP, Azarova AM, Tsai YC, Ban Y, and Liu LF (2007) Topoisomerase IIbeta mediated DNA double-strand breaks: implications in doxorubicin cardiotoxicity and prevention by dexrazoxane. *Cancer Res* **67:**8839-8846.

McPherson E, Archila R, Schein PS, Tew KD, and Mhatre RM (1984) Preclinical pharmacokinetics, disposition and metabolism of ICRF-187. *Proceedings of the American Association for Cancer Research* **25:**362-362.

Mhatre RM, Tew KD, Vanhennik MB, Waravdekar VS, and Schein PS (1983) Absroption, distribution and pharmacokinetics of ICRF-187 in dogs. *Proceedings of the American Association for Cancer Research* **24:**290-290.

Popelova O, Sterba M, Haskova P, Simunek T, Hroch M, Guncova I, Nachtigal P, Adamcova M, Gersl V, and Mazurova Y (2009) Dexrazoxane-afforded protection against chronic anthracycline cardiotoxicity in vivo: effective rescue of cardiomyocytes from apoptotic cell death. *Brit J Cancer* **101:**792-802.

Rosing H, ten Bokkel Huinink WW, van Gijn R, Rombouts RF, Bult A, and Beijnen JH (1999) Comparative open, randomized, cross-over bioequivalence study of two intravenous dexrazoxane formulations (Cardioxane and ICRF-187) in patients with advanced breast cancer, treated with 5-fluorouracil-doxorubicin-cyclophosphamide (FDC). *Eur J Drug Metab Pharmacokinet* **24:**69-77.

Schroeder PE, Davidson JN, and Hasinoff BB (2002) Dihydroorotase catalyzes the ring opening of the hydrolysis intermediates of the cardioprotective drug dexrazoxane (ICRF-187). *Drug Metab Dispos* **30:**1431-1435.

Schroeder PE and Hasinoff BB (2002) The doxorubicin-cardioprotective drug dexrazoxane undergoes metabolism in the rat to its metal ion-chelating form ADR-925. *Cancer Chemother Pharmacol* **50:**509-513.

Schroeder PE and Hasinoff BB (2005) Metabolism of the one-ring open metabolites of the cardioprotective drug dexrazoxane to its active metal-chelating form in the rat. *Drug Metab Dispos* **33:**1367-1372.

Schroeder PE, Jensen PB, Sehested M, Hofland KF, Langer SW, and Hasinoff BB (2003) Metabolism of dexrazoxane (ICRF-187) used as a rescue agent in cancer patients treated with high-dose etoposide. *Cancer Chemother Pharmacol* **52:**167-174.

Schroeder PE, Patel D, and Hasinoff BB (2008) The dihydroorotase inhibitor 5-aminoorotic acid inhibits the metabolism in the rat of the cardioprotective drug dexrazoxane and its one-ring open metabolites. *Drug Metab Dispos* **36:**1780-1785.

Schroeder PE, Wang GQ, Burczynski FJ, and Hasinoff BB (2005) Metabolism of the cardioprotective drug dexrazoxane and one of its metabolites by isolated rat myocytes, hepatocytes, and blood. *Drug Metab Dispos* **33:**719-725.

Simunek T, Klimtova I, Kaplanova J, Mazurova Y, Adamcova M, Sterba M, Hrdina R, and Gersl V (2004) Rabbit model for in vivo study of anthracycline-induced heart failure and for the evaluation of protective agents. *European Journal of Heart Failure* **6:**377-387.

Simunek T, Sterba M, Popelova O, Kaiserova H, Adamcova M, Hroch M, Haskova P, Ponka P, and Gersl V (2008) Anthracycline toxicity to cardiomyocytes or cancer cells is differently affected by iron chelation with salicylaldehyde isonicotinoyl hydrazone. *Brit J Pharmacol* **155:**138-148.

Sterba M, Popelova O, Vavrova A, Jirkovsky E, Kovarikova P, Gersl V, and Simunek T (2013) Oxidative stress, redox signaling, and metal chelation in anthracycline cardiotoxicity and pharmacological cardioprotection. *Antioxidants & redox signaling* **18:**899-929.

Swain SM and Vici P (2004) The current and future role of dexrazoxane as a cardioprotectant in anthracycline treatment: expert panel review. *J Cancer Res Clin Oncol* **130:**1-7.

Tamai I (2013) Pharmacological and pathophysiological roles of carnitine/organic cation transporters (OCTNs: SLC22A4, SLC22A5 and Slc22a21). *Biopharm Drug Dispos* **34:**29-44.

Tetef ML, Synold TW, Chow W, Leong L, Margolin K, Morgan R, Raschko J, Shibata S, Somlo G, Yen Y, Groshen S, Johnson K, Lenz HJ, Gandara D, and Doroshow JH (2001) Phase I trial of 96-hour continuous infusion of dexrazoxane in patients with advanced malignancies. *Clin Cancer Res* **7:**1569-1576.

U.S. Food and Drug Administration. Center for Drug Evaluation and Research (CDER) (2001) Guidance for industry: Bioanalytical method validation.

van Dalen EC, Caron HN, Dickinson HO, and Kremer LC (2011) Cardioprotective interventions for cancer patients receiving anthracyclines. *Cochrane Database Syst Rev***:**CD003917; doi: 10.1002/14651858.CD003917.pub4.

Vavrova A, Jansova H, Mackova E, Machacek M, Haskova P, Tichotova L, Sterba M, and Simunek T (2013) Catalytic inhibitors of topoisomerase II differently modulate the toxicity of anthracyclines in cardiac and cancer cells. *PLoS One* **8:**e76676.

Vejpongsa P and Yeh ET (2014a) Prevention of anthracycline-induced cardiotoxicity: challenges and opportunities. J Am Coll Cardiol **64**:938-945.

Vejpongsa P and Yeh ET (2014b) Topoisomerase 2beta:A Promising Molecular Target for Primary Prevention of Anthracycline-induced Cardiotoxicity. *Clin Pharmacol Ther* **95:**45-52.

Vogel CL, Gorowski E, Davila E, Eisenberger M, Kosinski J, Agarwal RP, and Savaraj N (1987) Phase I clinical trial and pharmacokinetics of weekly ICRF-187 (NSC 169780) infusion in patients with solid tumors. *Investigational new drugs* **5:**187-198.

Wiseman LR and Spencer CM (1998) Dexrazoxane. A review of its use as a cardioprotective agent in patients receiving anthracycline-based chemotherapy. *Drugs* **56:**385-403.

Footnotes

Eduard Jirkovský and Anna Jirkovská contributed equally to this study.

This work was supported by the Czech Science Foundation [Grant n. 13-15008S], the Charles University Grant Agency [Grant n. 1324214], and the Charles University Research Program PRVOUK [Grant n.P37/5].

Figure Legends

Figure 1: Chemical structures of dexrazoxane, intermediates B and C, and ADR-925.

Figure 2: Conversion of DEX to ADR-925 and their distribution in isolated neonatal rat cardiomyocytes.

A) DEX and ADR-925 concentrations in the cell culture media during a 24-hour incubation of DEX (100 μM) in the presence (full symbols) or absence (empty symbols) of NVCM. **B)** Intracellular concentrations of DEX and ADR-925 during a 24-hour incubation of NVCM with 100 μM DEX (blue circles and red boxes) or ADR-925 (green boxes). **C)** Assay of influence of the active transport on ADR-925 uptake into NVCM. Incubation of NVCM with ADR-925 (100–1000 μM) under physiological (37 °C, circles) and decreased temperature (4 °C, boxes). **D)** The effect of NVCM lysate (full symbols) on DEX conversion to ADR-925 during a 24-hour incubation compared to ADS buffer (empty symbols). All experiments were performed with cell density of 4.8×10^6 cells (n = 4). "*" – statistical significance determined by One-Way ANOVA on Ranks with Dunn's post hoc test ($p \leq 0.01$).

Figure 3: Mean plasma concentration-time profiles of drugs under study after single- dose administration of DEX and ADR-925 to rabbits.

A) Plasma concentration-time profiles of DEX and ADR-925 after single-dose administration of DEX (60 mg/kg, *i.p.*). **B)** Plasma concentration-time profile of ADR-925 after single-dose administration of ADR-925 (60 mg/kg, 30 minutes *i.v.* infusion). Data are presented as the mean ± SD.

JPET Fast Forward. Published on December 22, 2017 as DOI: 10.1124/jpet.117.244848
This article has not been copyedited and formatted. The final version may differ from this version.

Figure 4: Cumulative urinary excretion of studied drugs.

A) Cumulative urinary excretion of DEX (circles) and ADR-925 (boxes) after single-dose administration of DEX (60 mg/kg, *i.p.*). **B)** Cumulative urinary excretion of ADR-925 after single-dose administration of ADR-925 (60 mg/kg, *i.v.* inf.). Solid lines represent best fits from nonlinear regression, and circles and boxes are observed amounts.

Figure 5: Schematic representation of the selected pharmacokinetic models for DEX and ADR-925.

A) Two-compartmental model with first-order absorption for DEX after *i.p.* administration. **B)** Two-compartmental model for ADR-925 after *i.v.* infusion. **C)** Four-compartmental parent-metabolite model for DEX and ADR-925. k_a – absorption rate constant; V_1, V_2, V_3 and V_4– volumes of central and peripheral compartments for DEX and ADR-925; Q_{12} and Q_{34} – inter-compartmental clearances; Cl_R – renal clearance; Cl_{NR} – non-renal clearance; Cl_{other} –clearance describing other elimination pathways of DEX; A_U – cumulative urinary excretion.

Figure 6: Visual predictive performance and goodness-of-fit graphs of the four-compartment population model for DEX and ADR-925.

A) Plasma concentration-time profiles of DEX and **B)** ADR-925 after single-dose administration of DEX (60 mg/kg, *i.p.*). **C)** Scatter plots of the observed vs. individual predicted concentrations for DEX and **D)** ADR-925. **E)** Cumulative urinary excretion of DEX and **F)** ADR-925 after single-dose administration of DEX (60 mg/kg, *i.p.*). The solid lines and shaded

areas represent the median predictions and the 90 % prediction intervals. The crosses are observed concentrations.

Figure 7: Tissue concentrations of compounds under study after single-dose *i.p.* DEX administration to rabbits.

Tissue concentration-time profiles of DEX and its metabolite ADR-925 after single-dose administration of DEX (60 mg/kg, *i.p.*) in **A)** LV myocardium, **B)** liver and **C)** soleus muscle. Data are presented as the mean ± SD.

Figure 8: DEX incubation with rabbit tissue homogenate and plasma.

A) Incubation of DEX (100 μM) with different amount of LV myocardium homogenate or **B)** liver homogenate. Data are presented as the mean ± SD.

Figure 9: DEX incubation with rabbit plasma.

A) Incubation of DEX (100 μM) with fresh rabbit plasma. **B)** Theoretical portion of intermediates metabolites B and C determined by mass balance calculations during incubation of DEX (100 μM) with fresh rabbit plasma. Data are presented as the mean ± SD.

Tables

Table 1: Summary of pharmacokinetic parameters of DEX and ADR-925 in rabbits determined by non-compartmental analysis.

	C_{max} [μM]	T_{max} [h]	AUC_{tlast} [h·μM]	AUC_{tot} [h·μM]	L_z [h^{-1}]	$t_{1/2}$ [h]	MRT [h]	CL [$L \cdot h^{-1} \cdot kg^{-1}$]	$A_u(0-inf)$ [% of dose[a,b]]	CL_R [$L \cdot h^{-1} \cdot kg^{-1}$]	V_z [$L \cdot kg^{-1}$]	V_{ss} [$L \cdot kg^{-1}$]	$f_{DEX-ADR}$
NCA of geometric mean profiles from all animals (n = 20)*													
DEX†	337	0.17	838	851	0.35	2.0	2.8	0.26	35.5	0.093	0.76	0.74	0.11
ADR-925 after DEX	35.6	0.75	242	264	0.24	2.9	5.3	NA	11.2[a]	0.092	NA	NA	NA
ADR-925‡ after ADR-925	557	0.50	832	834	0.41	1.7	1.8	0.24	89.5[b]	0.212	0.57	0.42	NA
***NCA of profiles from animals with 12-hour sampling (n = 5)** [c]*													
DEX†	424 (401-536)	0.18 (0.09-0.27)	797 (700-1140)	815 (710-1180)	0.34 (0.32-0.43)	2.1 (1.9-2.6)	2.8 (2.7-3.4)	0.28 (0.24-0.40)	34.0[a] (29.9-48.8)	0.095 (0.089-0.12)	0.81 (0.73-1.13)	0.768 (0.73-0.95)	0.11 (0.089-0.16)
	35.3	3.4	215	243	0.23	3.0	5.8	NA	10.3[a]	0.11	NA	NA	NA

ADR-925 after DEX	(31.8-48.6)	(0.70-6.10)	(210-250)	(235-294)	(0.21-0.32)	(2.7-4.1)	(5.2-7.8)	NA	(8.7-15.5)	(0.098-0.14)	NA	NA	NA
ADR-925‡ after ADR-925	581 (495-681)	0.5[d] NA	900 (820-987)	902 (821-990)	0.41 (0.34-0.49)	1.7 (1.4-2.0)	1.7 (1.5-2.0)	0.22 (0.20-0.24)	97.3[b] (91.9-104)	0.21 (0.202-0.22)	0.54 (0.45-0.64)	0.38 (0.34-0.42)	NA NA

** 4 groups each of 5 animals terminated in 0.5, 3, 6 and 12 hours after a drug administration. For DEX, the estimates of clearances and volumes were obtained assuming F = 1. Cumulative urinary excretion in % of: a - the dose of DEX, b - the dose of ADR-925, c - the data are presented as geometric means and antilogarithms of (means ± SD, ln-data); d - T_{inf} =0.5 h; † - i.p. bolus (60 mg·kg^{-1}); ‡ - i.v. infusion (60 mg·kg^{-1}); NA - not applicable.*

Table 2: Summary of pharmacokinetic parameters determined by population modelling approach in rabbits.

		k_a [h^{-1}]	V_1 [$L \cdot kg^{-1}$]	V_2 [$L \cdot kg^{-1}$]	Q_{12} [$L \cdot h^{-1} \cdot kg^{-1}$]	V_3 [$L \cdot kg^{-1}$]	V_4 [$L \cdot kg^{-1}$]	Q_{34} [$L \cdot h^{-1} \cdot kg^{-1}$]	Cl_{NR} [$L \cdot h^{-1} \cdot kg^{-1}$]	Cl_R [$L \cdot h^{-1} \cdot kg^{-1}$]	$Cl_{DEX-ADR}$ [$L \cdot h^{-1} \cdot kg^{-1}$]	RVPC [%CV]
Model 1 - A two-compartment open model with first order absorption of DEX (after DEX i.p. bolus)[a]												
DEX	estimated	12.8	0.41	0.28	0.72	NA	NA	NA	0.25	0.11	NA	27
	[% RSE]	(20)	(4)	(14)	(22)				(14)	(12)		(7)
	ISV	81	5.8	53	73	NA	NA	NA	45	44	NA	NA
	[% RSE]	(18)	(77)	(20)	(22)				(25)	(24)		
Model 2 - A two-compartment open model for ADR-925 (after ADR-925 i.v. infusion)[b]												
ADR-925	estimated	NA	0.072	0.32	1.7	NA	NA	NA	NA*	0.24	NA	22
	[% RSE]		(8)	(2)	(21)					(4)		(9)
	ISV	NA	10.4	3.6	58	NA	NA	NA	NA*	10.1	NA	NA
	[% RSE]		(92)	(49)	(26)					(28)		
Model 3 - A four-compartment open model for DEX as parent compound and ADR-925 as metabolite												
DEX	estimated	15.3	0.45	0.27	0.57	NA	NA	NA	0.11	0.09	0.045	15
	[% RSE]	(20)	(3)	(12)	(16)				(14)	(8)	(9)	(6)
	ISV	81	7.7	50	60	NA	NA	NA	50	26	36	NA

	[% RSE]	(18)	(36)	(18)	(20)				(21)	(26)	(19)	
ADR-925	estimated	NA	NA	NA	NA	0.013	0.3	1.7	NA*	0.15	NA	22
	[% RSE]					(24)	(15)	(10)		(10)		(10)
	ISV	NA	NA	NA	NA	71	65	36	NA*	36	NA	NA
	[% RSE]					(29)	(17)	(23)		(21)		

*a - the estimates of clearances and volumes of distribution were obtained assuming F = 1 for i.p. administration of DEX; b - t_{inf} = 30 min; ISV - inter-subject variability expressed as percent of CV; RVPC – residual variability in plasma concentrations; % RSE - percent of relative standard error; NA - not applicable. * - Renal clearance was the sole elimination pathway for ADR-925 (urinary recovery of the infused dose achieved 98 ± 6 % in 5 animals with a 12-hour interval of collection). Schematic representation of the selected models is given in Fig. 4.*

Table 3: Estimated AUC of DEX and ADR-925 in selected tissues after administration of DEX to rabbits (60 mg/kg, i.p.).

Tissue	Compound	c [h·µM]	SE [h·µM]	95 % t-CI [h·µM]	AUC_{0-12} [h·µM]	Ratio of AUC_{0-12} tissue vs. plasma
LV myocardium	c_{DEX}	632	38	546–719	632	0.75
	$c_{ADR-925}$	111	13	80-142	111	0.46
Liver	c_{DEX}	589	31	521-657	589	0.70
	$c_{ADR-925}$	123	12	94-152	123	0.51
Soleus	c_{DEX}	531	38	440-622	531	0.63
	$c_{ADR-925}$	153	15	116-189	153	0.63

AUCs were estimated by batch method from all animals in 4 groups each of 5 animals terminated in 0.5, 3, 6 and 12 hours after DEX administration (60 mg/kg, i.p.).

Figures

Figure 1:

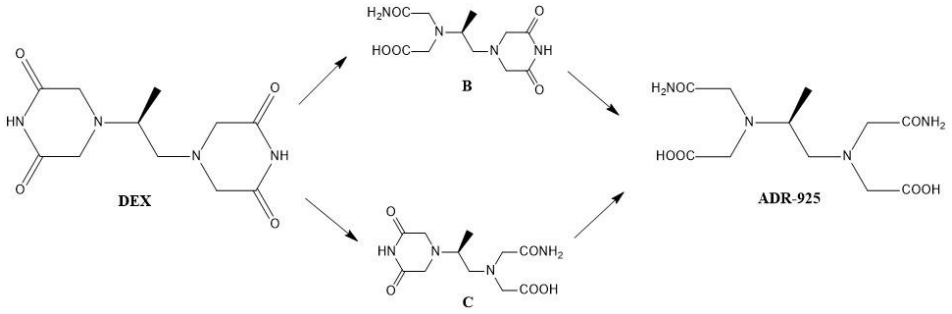

Figure 2:

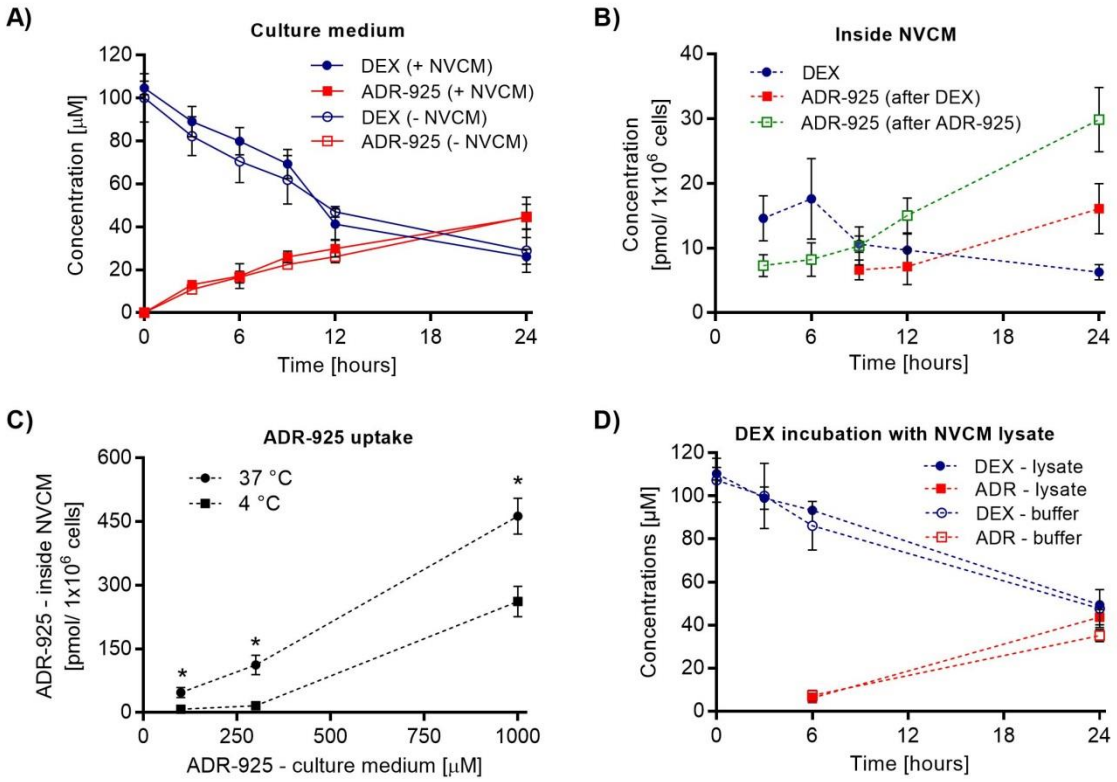

JPET Fast Forward. Published on December 22, 2017 as DOI: 10.1124/jpet.117.244848
This article has not been copyedited and formatted. The final version may differ from this version.

Figure 3:

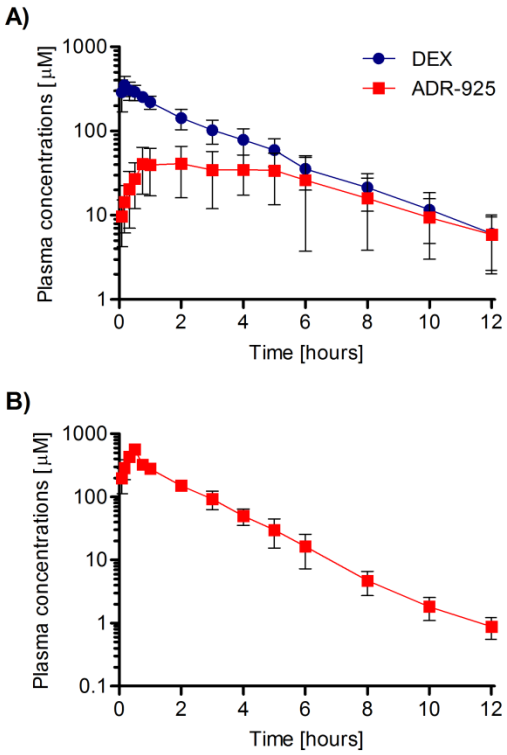

Figure 4:

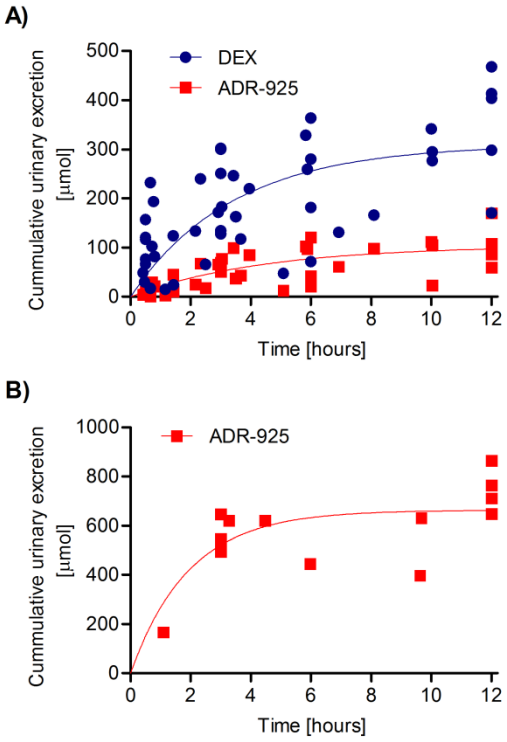

JPET Fast Forward. Published on December 22, 2017 as DOI: 10.1124/jpet.117.244848
This article has not been copyedited and formatted. The final version may differ from this version.

Figure 5:

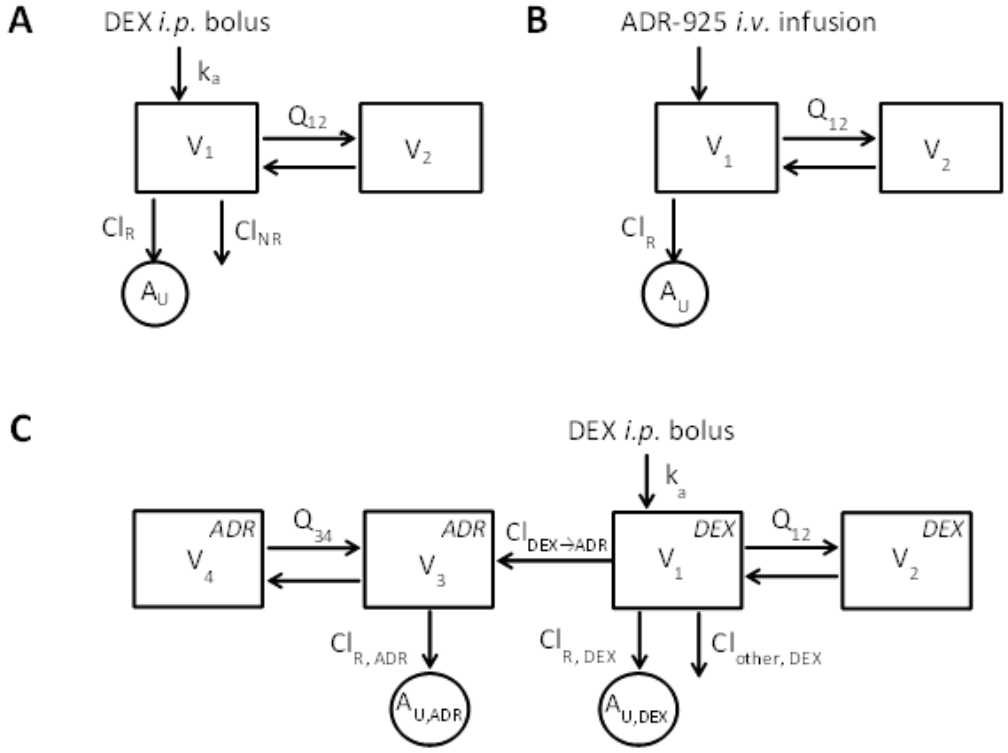

JPET Fast Forward. Published on December 22, 2017 as DOI: 10.1124/jpet.117.244848
This article has not been copyedited and formatted. The final version may differ from this version.

Figure 6:

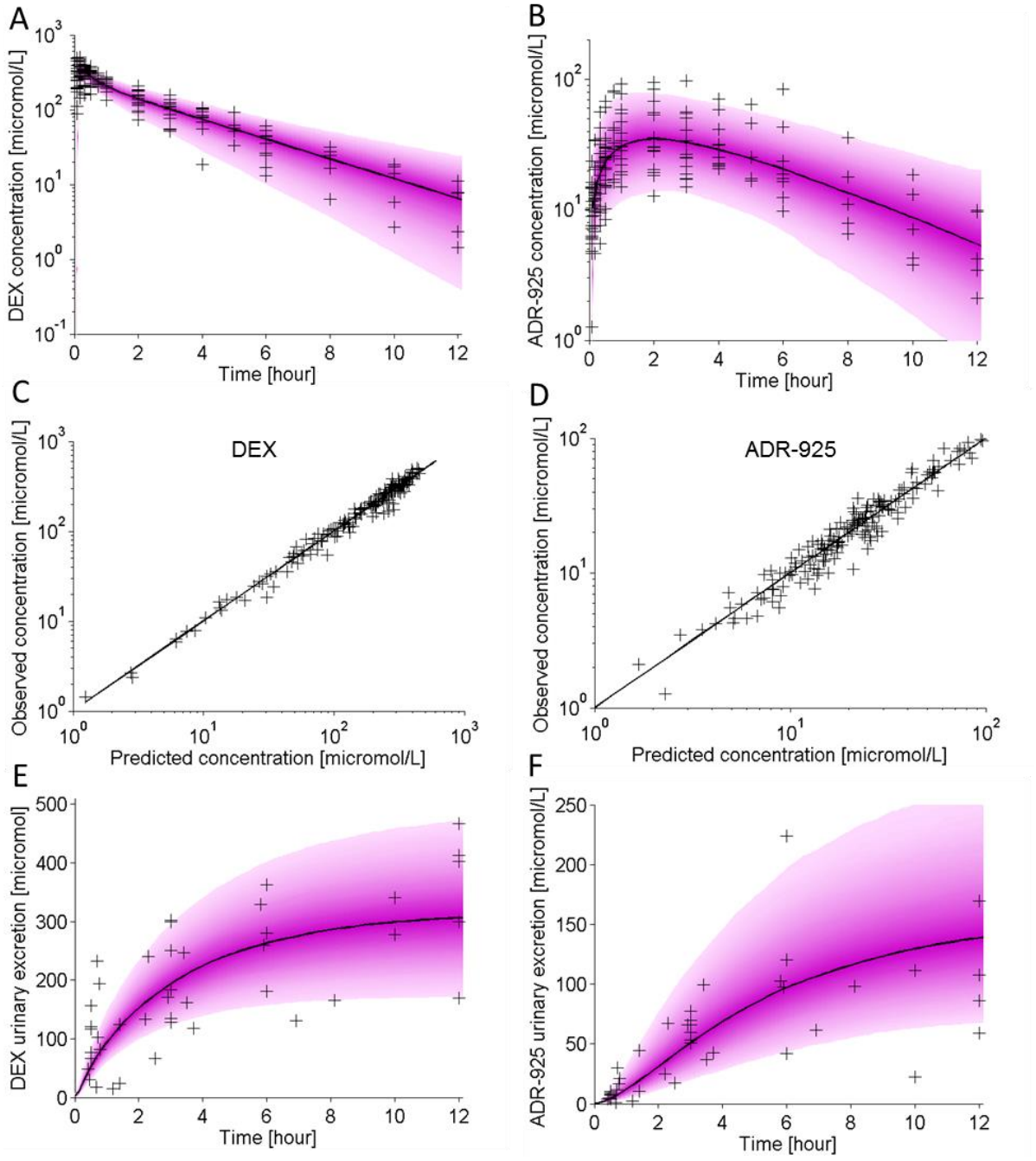

JPET Fast Forward. Published on December 22, 2017 as DOI: 10.1124/jpet.117.244848
This article has not been copyedited and formatted. The final version may differ from this version.

Figure 7:

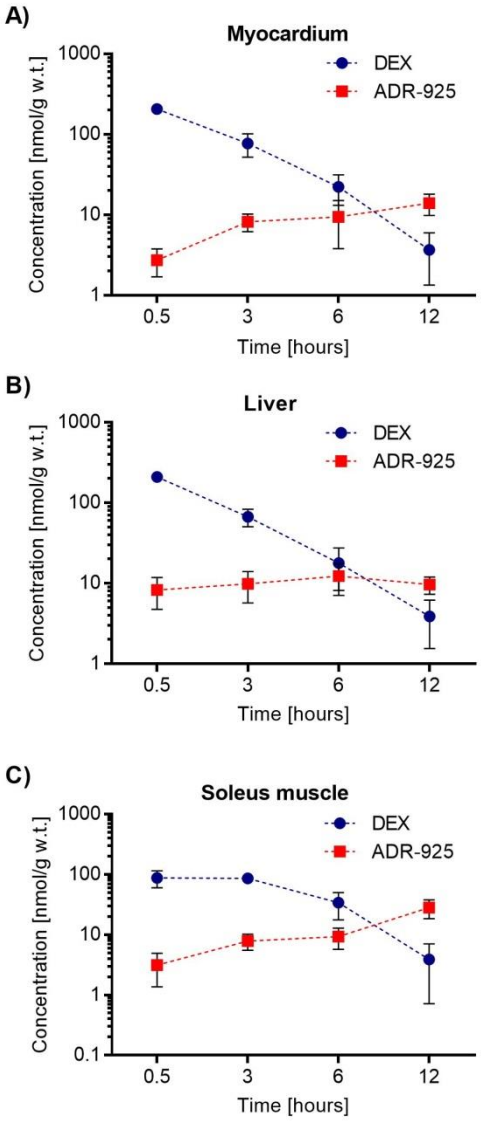

Figure 8:

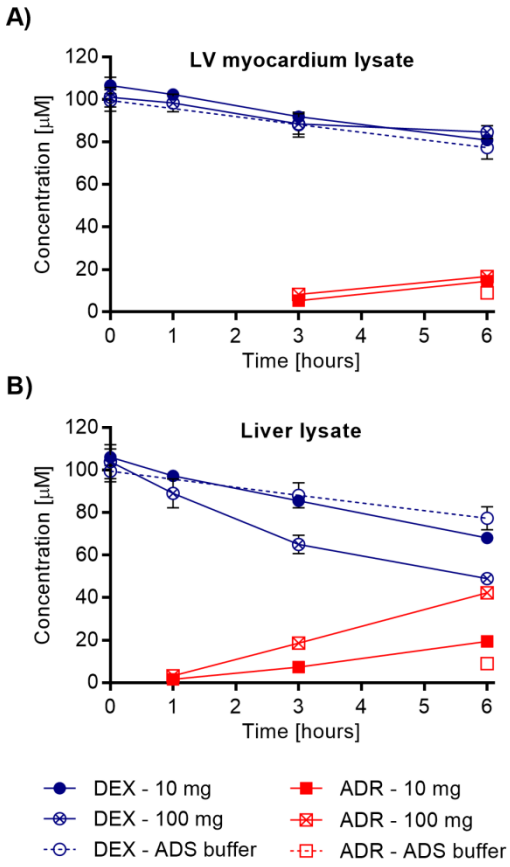

Figure 9:

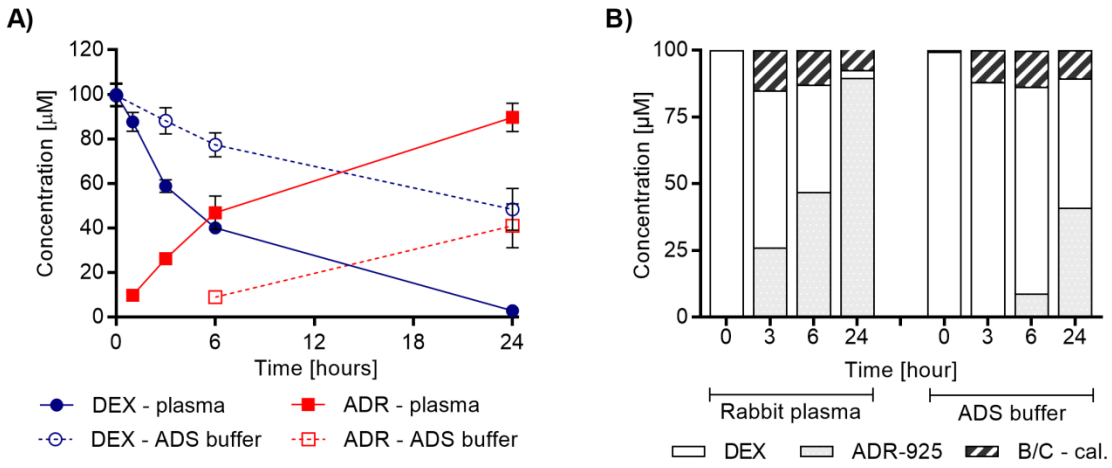

Pharmacokinetics of the cardioprotective drug dexrazoxane and its active metabolite ADR-925 with focus on cardiomyocytes and the heart

Eduard Jirkovský, Anna Jirkovská, Jan Bureš, Jaroslav Chládek, Olga Lenčová, Ján Stariat, Zuzana Pokorná, Galina Karabanovich, Jaroslav Roh, Petra Brázdová, Tomáš Šimůnek, Petra Kovaříková and Martin Štěrba

Supplemental Figures

Supplemental Figure 1: Visual predictive performance and goodness-of-fit of the two-compartment population models for drugs under study.

A) Plasma concentration-time profile of DEX after single-dose administration of DEX (60 mg/kg, *i.p.*) and **B)** ADR-925 after single-dose administration of ADR-925 (60 mg/kg, *i.v.* infusion). **C)** Scatter plots of the observed vs. individual predicted concentrations for DEX and **D)** ADR-925. The solid lines and shaded areas represent the median predictions and the 90 % prediction intervals. The crosses are observed concentrations.

Supplemental Figure 2: Correlation analyses of end-point plasma and individual tissue concentrations of drugs under study in rabbits.

Correlation coefficients and statistical significances were determined by Pearson (**A**) and Spearman (**B**-**F**) correlation analyses and by linear regression analysis.

Supplemental Figure 1:

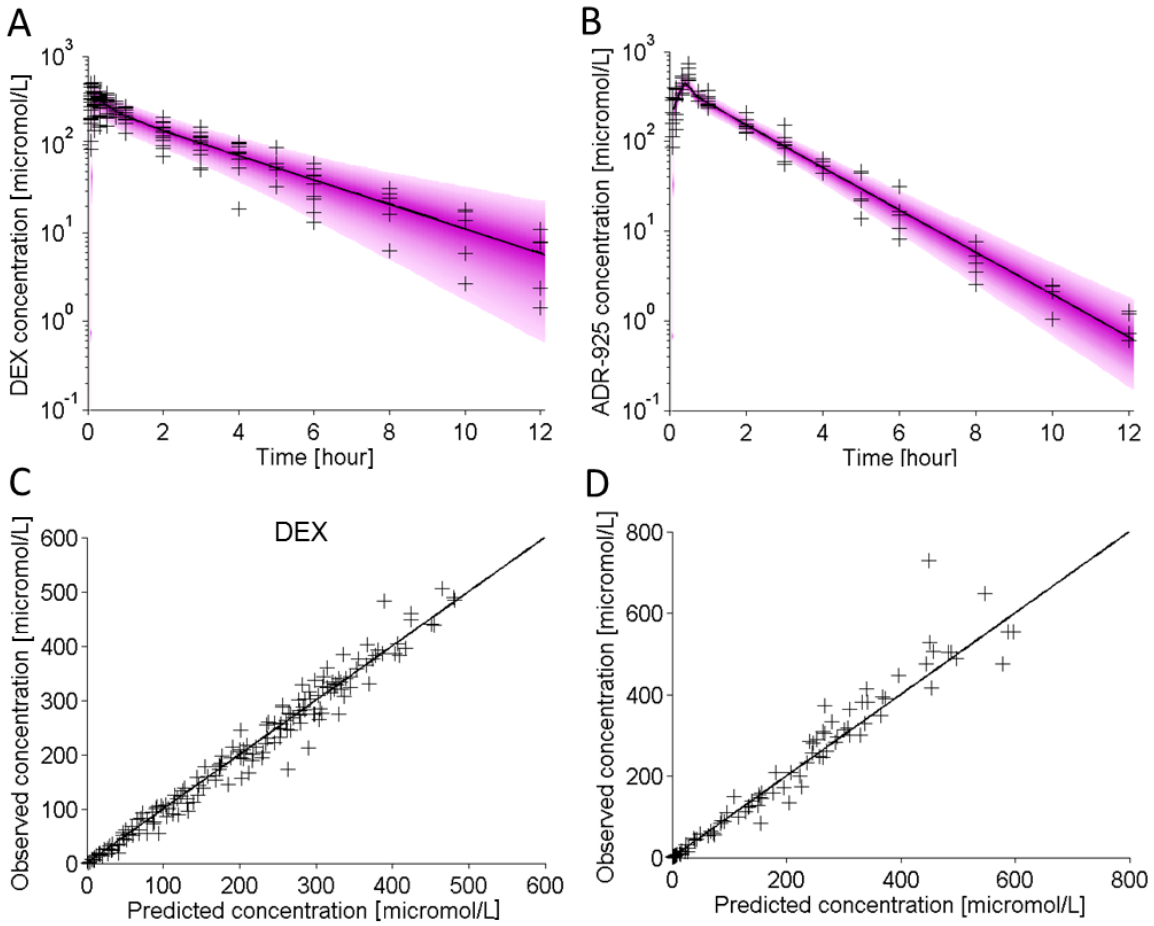

Supplemental Figure 2:

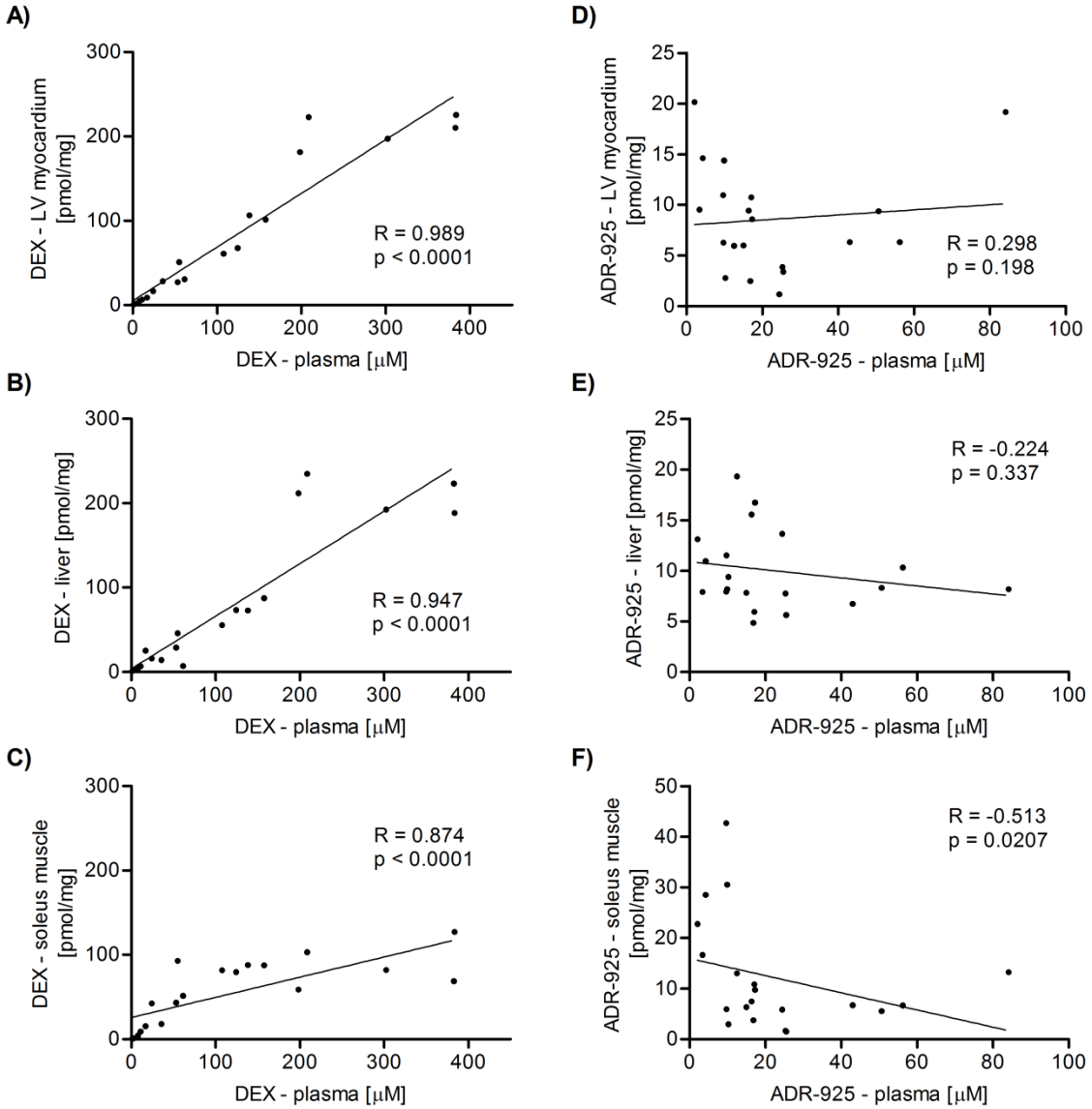

Pharmacokinetics of the cardioprotective drug dexrazoxane and its active metabolite ADR-925 with focus on cardiomyocytes and the heart

Eduard Jirkovský, Anna Jirkovská, Jan Bureš, Jaroslav Chládek, Olga Lenčová, Ján Stariat, Zuzana Pokorná, Galina Karabanovich, Jaroslav Roh, Petra Brázdová, Tomáš Šimůnek, Petra Kovaříková and Martin Štěrba

Supplemental Method

Preparation of the racemic form of ADR-925 (ICRF-198)

The racemic form of ADR- 925 (ICRF-198) (MW = 304 g/mol) was prepared in house according to the procedure described previously (Kovarikova et al., 2011). Briefly, razoxane was prepared from (±)-1,2-diaminopropan-*N*,*N*,*N'*,*N'*-tetraacetic acid via known method (Bis diketopiperazines: Creighton, A. M. US3941790, 1976.) Razoxane (10 g, 37.3 mmol) was stirred in 0.5 M aqueous NaOH (149.2 mL) at rt for 24 hours. Upon completion, the solution was acidified to pH 5-6 with Amberlyst 15, filtered, and the filtrate was evaporated to dryness under vacuum. The resulting solid was further dried over P_2O_5 under vacuum in a dessicator for 7 days. Yield: 91% (11 g) as a white solid. The product was obtained as a (±)-ADR-925 monohydrate. Anal. Calcd for $C_{11}H_{22}N_4O_7$: C, 40.99; H, 6.88; N, 17.38. Found: C, 40.52; H, 6.62; N, 17.1. ^{1}H NMR (300 MHz, D_2O) δ 3.87 – 3.74 (m, 3H), 3.66 (d, *J* = 3.7 Hz, 1H), 3.62 – 3.54 (m, 2H), 3.55 – 3.44 (m, 3H), 3.26 (dd, *J* = 14.6, 4.0 Hz, 1H), 2.97 (dd, *J* = 14.6, 11.7 Hz, 1H), 1.18 (d, *J* = 6.6 Hz, 3H). ^{1}H NMR (500 MHz, DMSO) δ 7.74 (s, 1H), 7.59 (s, 1H), 7.21 (s, 1H), 7.16 (s, 1H), 3.25 – 2.92 (m, 8H), 2.79 (br s, 1H), 2.55 – 2.50 (m, 1H), 2.31 (br s, 1H), 0.83 (d, *J* = 6.4 Hz, 3H). ^{13}C NMR (75 MHz, D_2O) δ 175.17, 174.14, 173.85, 171.94, 57.10, 56.98, 56.69, 56.61, 53.91, 53.83, 10.64. ^{13}C NMR (126 MHz, DMSO) δ 173.71, 173.08, 57.81 (broad), 56.86 (broad), 54.15 (broad), 11.88.